TECHNICAL PAPER

Analytical and Numerical Analyses of the Support System for a Large-span Tunnel in Challenging and Seismically Active Ground Conditions

Ebu Bekir Aygar[1] · Servet Karahan[2] · Suat Gullu[2] · Candan Gokceoglu[3]

Abstract

The Dogancay T1 tunnel, projected within the scope of the Ankara-Istanbul high-speed train project, is being excavated entirely through clay and cohesionless units and is located in the North Anatolian Fault Zone (NAFZ). To determine the support system in the tunnel, innovative approaches require investigation through analytical and numerical methods to evaluate their suitability. The present study investigates rigid support systems, including the intermediate lining and pre-support excavation techniques in the new Austrian tunneling method (NATM), with 3D numerical analyses. The tunnel is in a seismically active zone, and the study also addresses the seismic sustainability of the proposed support system. The results of analyses showed that the proposed excavation and support system can be successfully implemented in the Dogancay T1 tunnel. The case study provides guidelines for investigating tunnel excavation and support systems in poor ground conditions in tectonically active zones.

Keywords Intermediate lining · Tunnel in cohesionless soil · 3D numerical analysis · Rigid support system · Analytical solution · Deformations · Face support · Dogancay tunnel · NATM

✉ Candan Gokceoglu
cgokce@hacettepe.edu.tr

[1] Fugro Sial Geosciences Consulting Engineering Ltd, Ankara, Türkiye

[2] Directorate General of Turkish Railway System, Ankara, Türkiye

[3] Department of Geological Engineering, Hacettepe University, Beytepe, Ankara, Türkiye

1 Introduction

The Dogancay T1 tunnel in the north-western part of Türkiye lies between km: 124 + 660–127 + 548 of the Ankara-Istanbul high-speed train project, with a total length of 2888 m. Tunnel excavation was occurring from both tunnel entrances as of 2021. The longitudinal slope of the tunnel is 2.1%, the entrance altitude is 60 m, and it rises to 120 m at the exit. A significant part of the tunnel route passes through extremely poor lithological units and is within the North Anatolian Fault Zone, one of the most active fault zones in the World. According to the NATM (new Austrian tunneling method) support classes, the tunnel is excavated completely in squeezing and flowing rock classes. In these types of rock classes, the bench pilot tunnel system is used to stabilize the tunnel, but using this method, the tunnel excavation system is a very complex and difficult construction process.

For a long period, tunnels in weak grounds have been the subject of many studies (Dalgic, 2002; Lee and Schubert, 2008; Cao et al., 2018, 2020; Luo et al., 2018; Aksoy et al., 2016; Sakcali and Yavuz, 2019; Aygar and Gokceoglu, 2020 and Aygar and Gokceoglu 2021a). In recent years, depending on technological developments, tunneling with tunnel boring machines (TBMs) has been successfully applied in long tunnels excavated in weak rock and/or under adverse geological conditions (Farrokh and Rostami, 2009; Yagiz et al., 2009; Armaghani et al., 2016; Swannell et al., 2016; Adoko et al., 2017; Maleki and Dehnavi, 2018; Hasanpour et al. 2018; Eftekhari and Aalianvari, 2019; Alp and Apaydin, 2019; Komu et al., 2020). However, the NATM is still preferred in extremely heterogeneous geological environments with high uncertainty and relatively short tunnels. NATM is not a tunneling method but an approach covering all general principles of tunneling (Aygar, 2020). The NATM introduced in the 1960s by (Rabcewicz 1964a, Rabcewicz 1964b and Rabcewicz 1965) aims to maximize the self-carrying capacity of overburden. Considering this principle, several tunnels have been successfully completed (Barton, 2017; Taromi et al., 2017; Song and Yoo, 2018; Zhang et al., 2018a, b; Niedbalski et al., 2018; Li et al., 2019; Agbay and Topal, 2020; Satici and Topal, 2021; Aygar and Gokceoglu, 2021b and c; Kong et al., 2021). Aygar (2020) emphasized a wide range of opinions that each tunnel brings with a site-specific method, and the results obtained in a tunnel tend to serve as a guide for other tunnels. This statement is valuable for the development of geotechnical engineering and engineering geology theories and practices. In addition, Bieniawski (1989) defined the objectives of rock mass classification systems as "*relate the experience of rock conditions at one site to the conditions and experience encountered at others.*" These considerations clearly reveal the importance of new case studies for the development of rock engineering, geotechnical engineering, and engineering geology. Tunneling is of common interest in rock engineering, geotechnical engineering, and engineering geology.

The necessity of a rigid support system in large diameter tunnels excavated in weak grounds is important. The rigid or non-deformable support system of tunnels to be excavated in squeezing and swelling ground conditions is preferred (Aksoy and Onargan, 2010; Aksoy et al., 2010, 2012 and Aksoy et al. 2014). The Bolu tunnel was initially designed according to NATM principles and a flexible outer arch

principle (Aygar 2020, 2007 and Aygar and Gokceoglu 2020). However, deformations up to 1.2 m occurred in the tunnel (Aygar 2020, Aygar and Gokceoglu 2020), and this section of the tunnel completely collapsed with the occurrence of the November 12, 1999 Düzce earthquake. In the re-design stage, it was seen that tunnel stability could not be ensured with a flexible outer arch principle, and the project was started with a rigid outer arch principle (Aygar 2020). An intermediate (Bernold) lining was applied in short fault zones and flysch series, and the bench pilot tunnel method, which is a more rigid support system, was used in long fault zones (Aygar, 2020).

Intermediate linings have been used worldwide since the 1970s. They are preferred when a rigid support system is required immediately after excavation. Thus, the loosening and plastic behavior that may occur in the tunnel are prevented, and the support systems can be completed (EWI and WIRKIR, 1972). The aim is to minimize plastic zones that may form in the tunnels with the rigid support system applied as an intermediate lining in the logic of the intermediate lining in the Doğançay T1 tunnel.

The seismic behavior of the tunnels is very important for the tunnels constructed in the high seismic zone. Some damages in tunnels during the 1995 Kobe, Japan earthquake, the 1999 Chi-Chi, Taiwan earthquake, and the 1999 Kocaeli, Türkiye earthquake (Hashash et al. 2001) were encountered. Suitable seismic design of shallow tunnels constructed in weak grounds, especially in earthquake zones, has emerged as an inevitable requirement.

Increasing population and demand for human transport have resulted in the need for new high-speed railways and highways. However, due to the geometrical constraints of high-speed railways and highways, it is not always possible to avoid problematic areas when determining routes. In Turkey, which is located in the Alpine-Himalayan earthquake belt, the construction of many high-speed railway and highway projects has started in recent years. Due to the extremely complex geological structure, it is not possible to avoid active faults, landslide areas and/or extremely weak lithological units when determining a railway or highway route in Turkey. Bilgin (2016) emphasized these difficulties as follows: "*The geology of Türkiye is very complex and major Northern and Eastern Faults including minor faults associated with these faults create tremendous problems.*" Therefore, in recent years, many railway and highway tunnels in Turkey have been constructed under difficult geological conditions (Dalgic, 2002 and Dalgic 2003; Aydin et al., 2004; Aksoy et al., 2010, 2012 and Aksoy et al. 2014; Bilgin and Algan, 2012; Ozcelik, 2016; Bilgin and Ates, 2016; Kaya and Bulut, 2019; Komu et al., 2020; Aygar and Gokceoglu, 2020, 2021a, b, and Aygar and Gokceoglu 2021c; Apaydin, 2021; Satici and Topal, 2021; Bilgin and Acun, 2021).

The purposes of this study are to present an excavation-support design so that tunnel construction in complex geological conditions can be completed safely and to investigate the proposed excavation-support system with 3D numerical analysis. In accordance with the purpose of the study, the geological-geotechnical properties of the tunnel route are revealed, the excavation-support system is described, and 3D numerical analyses are performed. Subsequently, the results obtained are discussed in terms of tunneling practice.
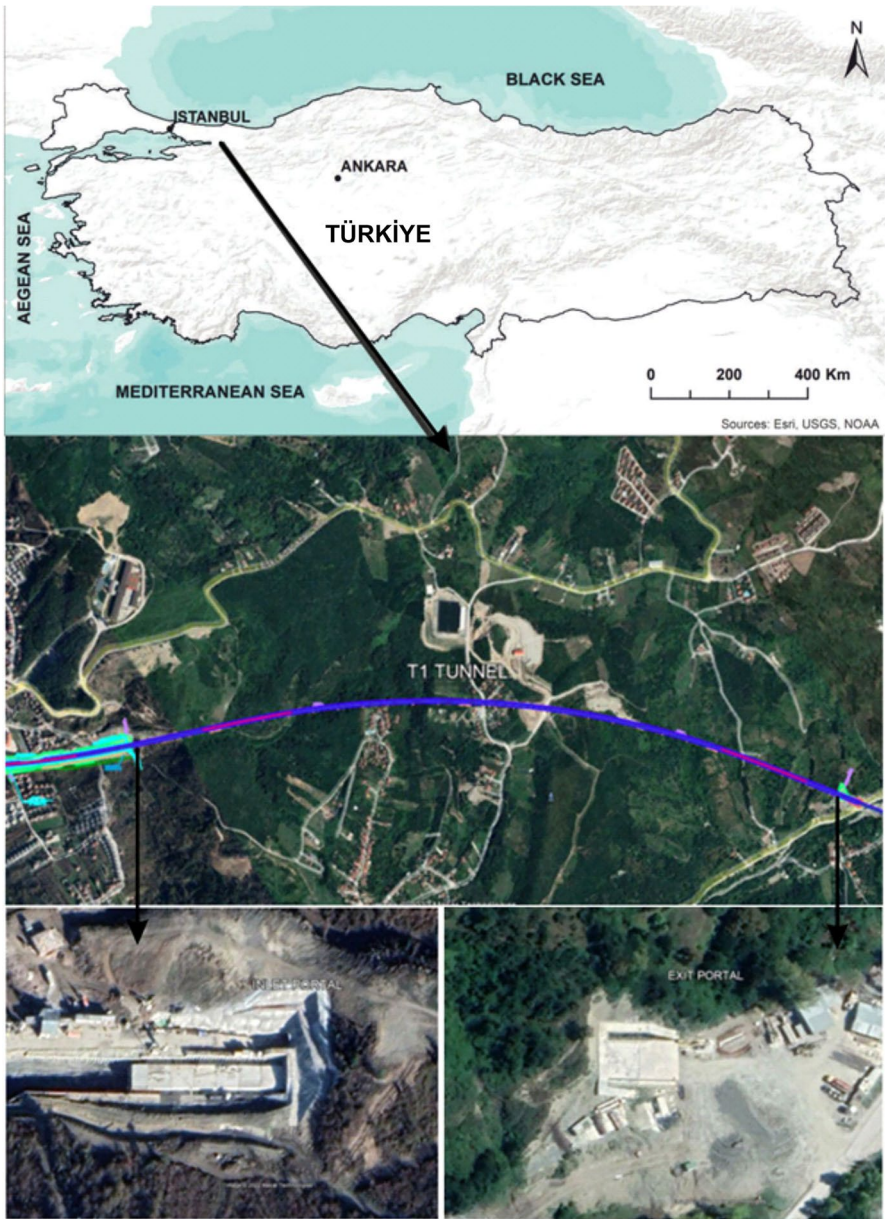
Fig. 1 Map portraying the location of the T1 tunnel and portal plan

2 Location and Specification of the Tunnel

The location map of the Dogancay T1 tunnel is given in Fig. 1, and the typical section of the tunnel is given in Fig. 2. As the finished dimensions of the tunnel, the
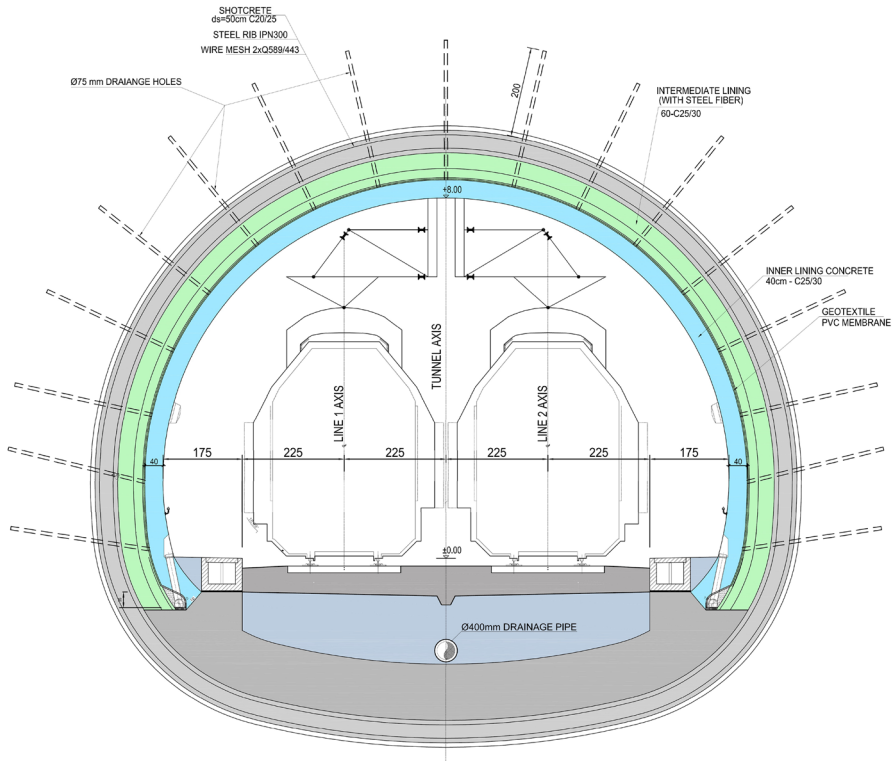
Fig. 2 Tunnel typical cross-section (Fugro Sial, 2019b)

tunnel height is 8.0 m, and the width is 12.5 m. In tunnel excavation, the width is 15.5 m, and the excavation height is 13.8 m. The tunnel overburden height varies from 30 to 140 m.

As shown in Fig. 3, the T1 tunnel is located in the eastern Marmara region. The region exhibits highly active tectonism. The landforms observed in the region developed under the influence of the Neotectonic period. These landforms are observed as high mountain belts, tectonic depression basins, and valleys located along fault segments. The North Anatolian Fault Zone (NAFZ), which forms the plate boundary, plays an important role in the formation of the morphology of the region. The NAFZ, which passes through the study area in the east–west direction, has been effective in the development of the structural and palaeographic evolution of the region during the Neotectonic period (Emre et al., 1998; Fugro Sial, 2019a). Due to these characteristics of the region, active faults and landslides are common in the region (Fig. 3). In addition to these adverse conditions, the lithological units forming the tunnel route are extremely weak.

The tunnel passes through Plio-Quaternary sediments on the southern boundary of the tectonically controlled basin. These sedimentary units form a soft
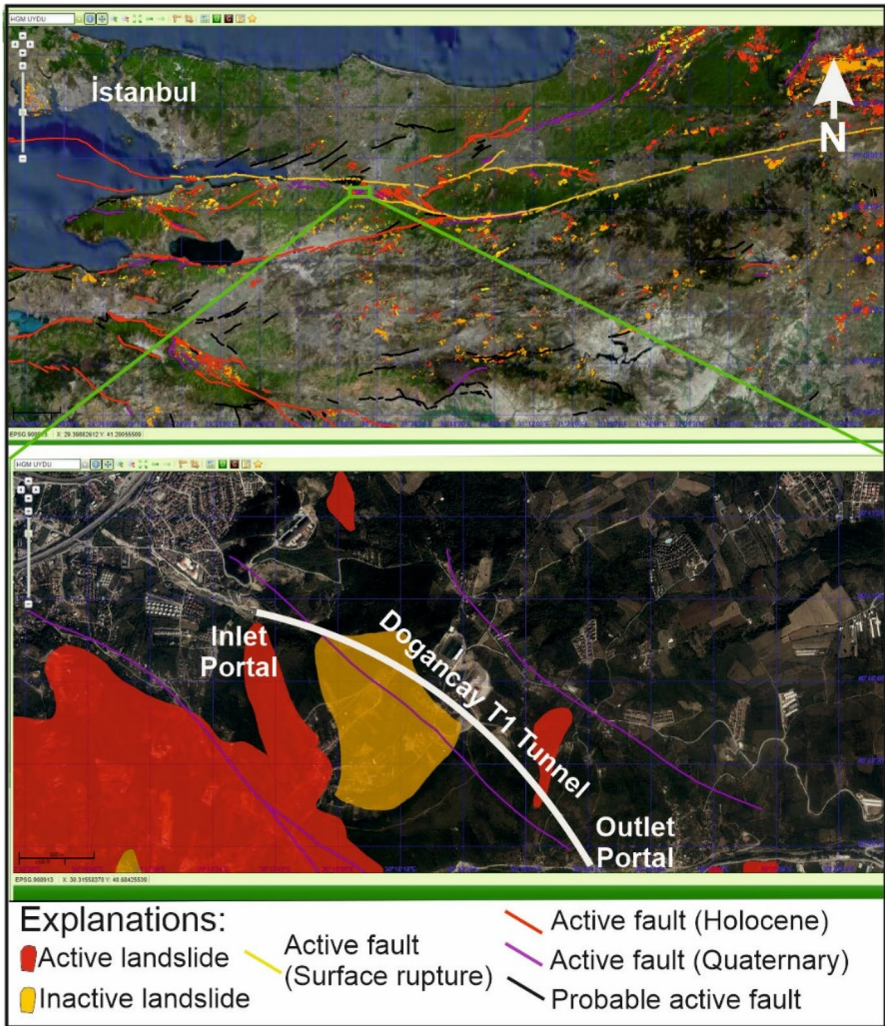
Fig. 3 Landslides and active faults around the T1 tunnel route (MTA, 2021)

topography reaching approximately 300 m above sea level on the north side of the steep morphology formed by the Armutlu-Almacık tectonic block. Yildirim and Tuysuz (2017) stated that the Almacık Block is one of the most pronounced push-up structures located between the major segments of the northern strand of the NAFZ, where it bifurcates in the eastern Marmara region.

The inlet portal of the tunnel, which has a total length of 2888 m, starts from a ridge at the west and reaches Akçay Valley at the east (Fig. 4). Along the tunnel, the thickness of the overburden reaches 70, 120, and 140 m at the ridges and decreases to 30–40 m at the valley crossings (Fig. 4). The entire T1 tunnel located within the
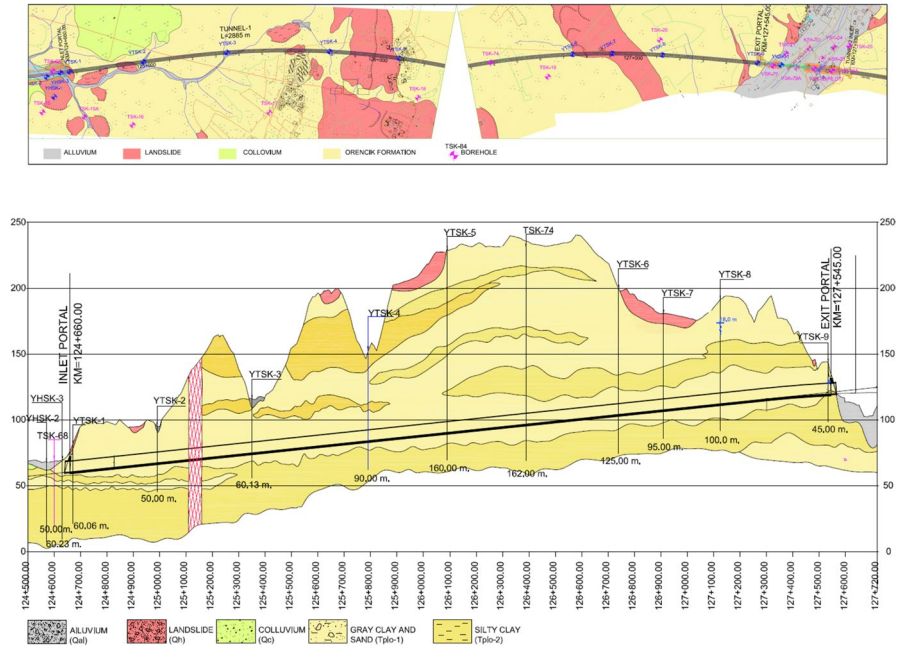
Fig. 4 Geological map and cross-section of the tunnel route (Fugro Sial, 2019a)

NAFZ (Fig. 3) is excavated in the Örencik Formation that consists of sand, silty sand, pebbly sand, and sandy gravel sediment units (Fig. 4).

Due to the geological and geotechnical conditions of the tunnel route, the stability of the support systems in the short term and the long term, and during an earthquake is critical. During a seismic event, the outer lining cannot carry extra loads; hence, an intermediate lining is selected to increase the bearing capacity of the lining.

In the analyses, a section with an overburden thickness of 30 m was chosen because it is the most critical section in terms of tunnel stability. In this section, the lithological units were investigated with the data obtained from the drillings performed by Fugro Sial (2019b) (Figs. 5, 6, and 7). In these drillings, at

Fig. 5 Mud, sand, and gravel units in the YTSK-1 borehole at the tunnel route (Fugro Sial, 2019a)
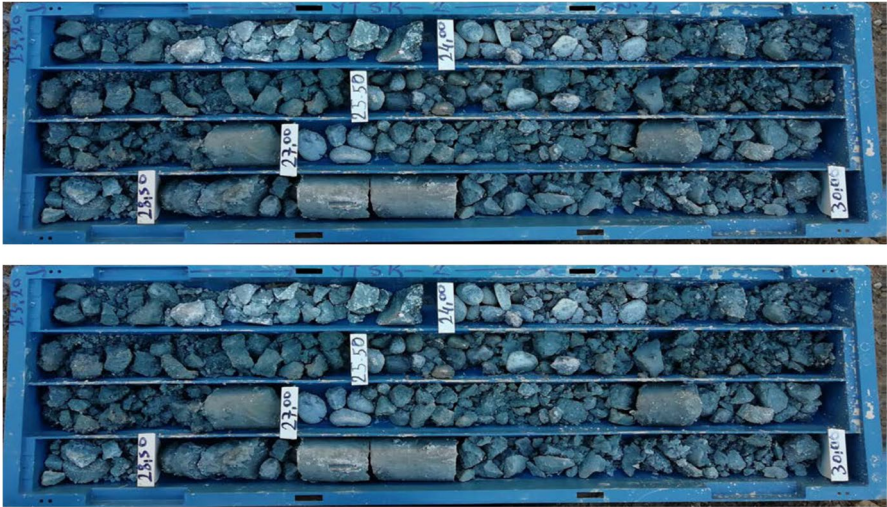
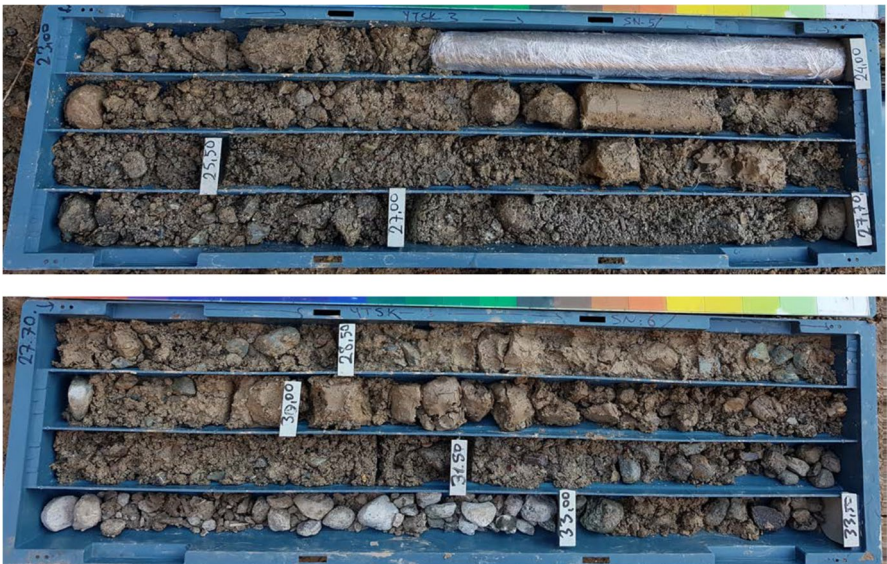**Fig. 6** Core-box photos for YTSK2 (Fugro Sial, 2019a)

Fig. 7 Core-box photos for YTSK3 (Fugro Sial, 2019a)

depths of 60 m and 50 m, in addition to the mud and sand levels, there are partly loose, pebble lenses up to meters in thickness. For the 60 m and 90 m overburden thickness sections, the analyses were carried out to compare different overburden effects on the tunnel stability. For 60 m of overburden thickness, the clay is selected completely as the lithological unit.

Table 1 Geotechnical parameters used in the analyses (Fugro Sial, 2019a)

Unit	Cohesion (kPa)	Internal friction angle (degree)	Deformation modulus (MPa)
Clay (short term)	200	0	200
Clay (long term)	50	22	200
Cohesionless units	5	35	150

The tunnel route contains clay, sand, silty-clayey sand, gravel, and sandy gravel sediments, all of which belong to the Örencik Formation (Fig. 4). The geotechnical design parameters of the units are given in Table 1 (Fugro Sial, 2019a) according to the results of the tests performed on the samples obtained from the YTSK-1, YTSK-2, and YTSK-3 (Figs. 5, 6, and 7). The unconsolidated-undrained (UU) and consolidated-drained (CU) triaxial tests and Atterberg limits were implemented in accordance with the procedures suggested by ASTM in Istanbul Kultur University.

3 Evaluation of Tunnel Support Systems

The methods used in determining tunnel support systems are divided into 3 main groups: empirical methods (Terzaghi 1946, Bieniawski, 1973, 1976 and Bieniawski, 1989; Barton et al. 1974 and Barton et al. 1980; Grimstad and Barton, 1993), analytical methods (Kirsch, 1898; Kastner, 1971; Hoek and Brown, 1980; Hoek, 2007 and Hoek 2012), and numerical methods (Moussaei et al., 2019; Panthi and Basnet, 2019; Aygar and Gokceoglu, 2021a).

Empirical approaches for the preliminary support design have been developed since the 1950s under the experience gained from mines and underground structures. These approaches, which started with Terzaghi (1946), continued with Bieniawski (1973, 1976, and Bieniawski, 1989), Rabcewicz (1964a), Barton et al. (1974), and Palmström 2000, Palmström 2009). These approaches contain extremely important and guiding data in terms of tunneling. All of these methods have certain limitations. For example, Terzaghi (1946) made classifications only according to steel ribs, while Bieniawski (1989) made classifications according to works in tunnels with a span of 5–12 m. Barton et al. (1974), on the other hand, developed his classification based on discontinuities, generally under high-quality rock masses. All of these classifications actually have a guiding basic principle in tunnel design. In all classifications, support systems are recommended by always giving a certain range in support systems. Therefore, these methods should be considered as the first step in tunnel design. The final support systems should be decided by analytical and numerical analyses.

Several researchers (Kirsch, 1898; Kastner, 1971; Sulem et al., 1987; Zhang et al., 2012a, 2012b, 2017; Zhang, 2018b; Wang et al., 2019; Hoek and Brown,

1980; Hoek, 2007 and Hoek 2012) have studied analytical solutions. According to this method, the environment is considered homogeneous and isotropic, and the tunnel is circular. In other words, all studies are carried out in an idealized environment. However, the unit through which the tunnel passes is not isotropic and homogeneous. Tunnels excavated conventionally are generally not circular. Although some researchers (i.e., Kargar et al., 2014; Wang et al., 2018) studied the analytical stress and displacement around non-circular tunnels, recently, analytical solutions have still some limitations.

Numerical analysis methods, on the other hand, have increased their application range in recent years and have been developed continuously. With numerical analysis, the current environment can be defined exactly, and the support systems to be applied in the tunnel can be described to the model exactly. Depending on the development of computer technology, tunnel methods, which are very complex, can also be modeled. Complex structures, such as multiple tunnels in mine galleries, junction structures in transportation tunnels, and metro stations, are modeled exactly, and the numerical analyses give much more accurate results. For this reason, numerical analysis is used as a crucial part of all tunnel projects today (Koçkar and Akgün, 2003; Akgün et al., 2014; Zou et al., 2019; Moussaei et al., 2019; Panthi and Basnet, 2019; Aygar and Gokceoglu, 2021a and Aygar and Gokceoglu 2021b). In numerical analysis methods, the most commonly applied methods involve finite elements, finite differences, discrete elements, and hybrid methods. Among these methods, finite elements are used relatively more widely (Das et al. 2017).

In this study, analytical solutions and numerical analyses were employed to assess the deformations and support system. In the first stage, analytical solutions were obtained, and then 3D numerical analyses were performed to assess the excavation and support systems. The lining system is suggested to be constructed in the following three phases:

a) Outer lining (steel rib, shotcrete, wire mesh, etc.)
b) Intermediate lining
c) Inner lining

The FLAC3D (Fast Lagrangian Analysis of Continua in 3 Dimensions) (Itasca, 2002) program was used in the numerical analysis. FLAC3D is a program that works with the finite difference method, and it gives the opportunity to model the tunnel in 3D and to use all supports in the model.

3.1 Tunnel Support Details

Figures 8 and 9 show a typical section and details of the support system applied in the tunnel, and Fig. 10 shows the longitudinal section of the tunnel support system. In addition, the details of the tunnel support elements are shown in Table 2. The tunnel excavation sequence is as follows: top heading, bench, and invert.

Before the excavation, the injection bolts were installed and grouted. After this application, 3 layers of 88.9 mm umbrellas were installed in the roof. After the top
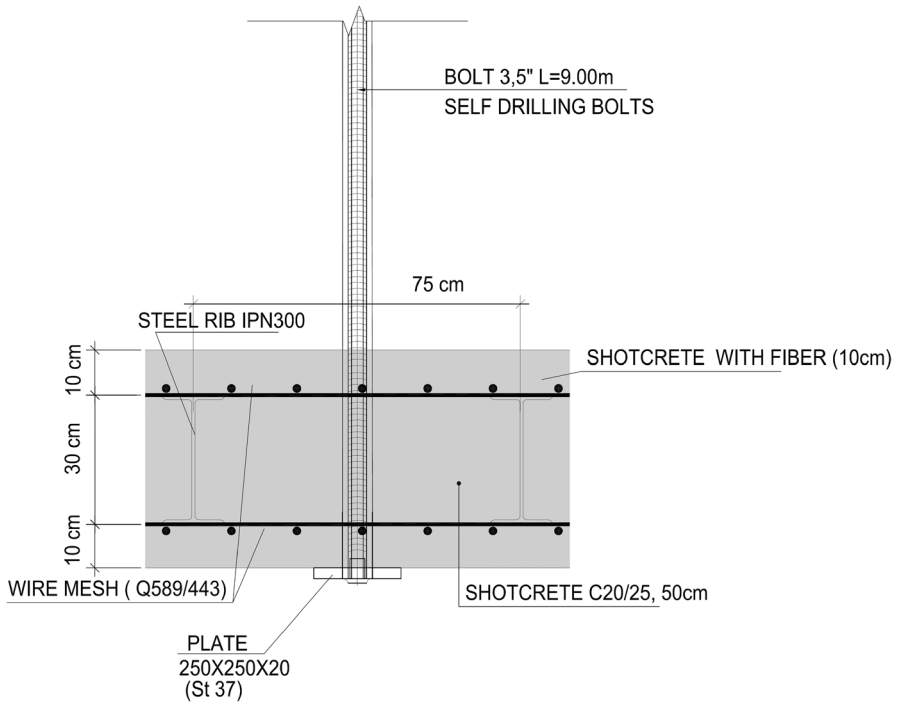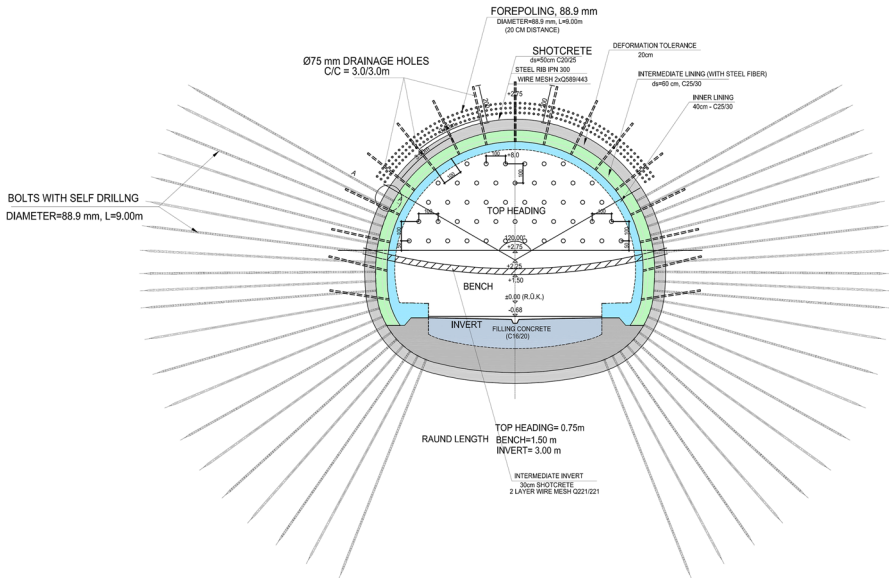
Fig. 8 Support details

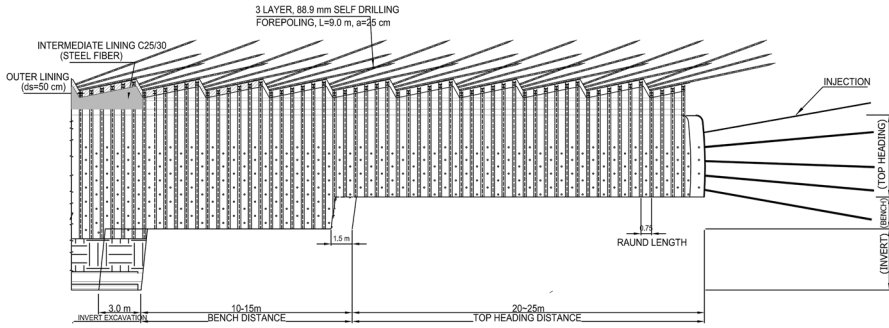**Fig. 9** Tunnel support system details (Fugro Sial, 2019b)

Fig. 10 Tunnel support system and excavation stages in the longitudinal section (Fugro Sial, 2019b)

Table 2 Properties of the support elements

Shotcrete, C20/25	50 cm
Steel rib	I300
Rock bolts	6–8 m, Self-drilling bolt, $d=89$ mm $P_{\text{ult}}=280$ kN
Fore-poling (3 layers)	9 m, 3.5 or 4″ 4.5 m overlap
Round length (m) Top heading/bench/invert	0.75/1.5/3.0
Wire mesh, Q221/221	2 layers
Face support Intermediate lining Inner lining	10 cm shotcrete/1 layer wire mesh 12 face bolts 60 m (C25/30) 40 m (C25/30)

heading excavation started at 0.75 m, in stage, an I300-type steel rib, 50 cm shot-crete, and 2 layers of wire mesh were installed.

This sequence involved 4 rounds in the top heading after the intermediate invert was installed. At the same time, bench excavation continued with the same supports as the top heading. This sequence continued at a distance of 20–25 m from the top heading and bench. After completing the 3-m bench excavation, the invert excavation was completed very close to the bench site. The ring closure was completed 30–40 m between the top heading and invert (Fig. 10). After this section, the intermediate lining was installed maximum 40 m behind the face. Therefore, this rigid support system allows minimum deformation along the tunnel.

3.2 Support System Construction

The support system construction stages are given in Fig. 11. In the first stage, umbrella and face bolts are installed; in the second stage, top heading excavation;
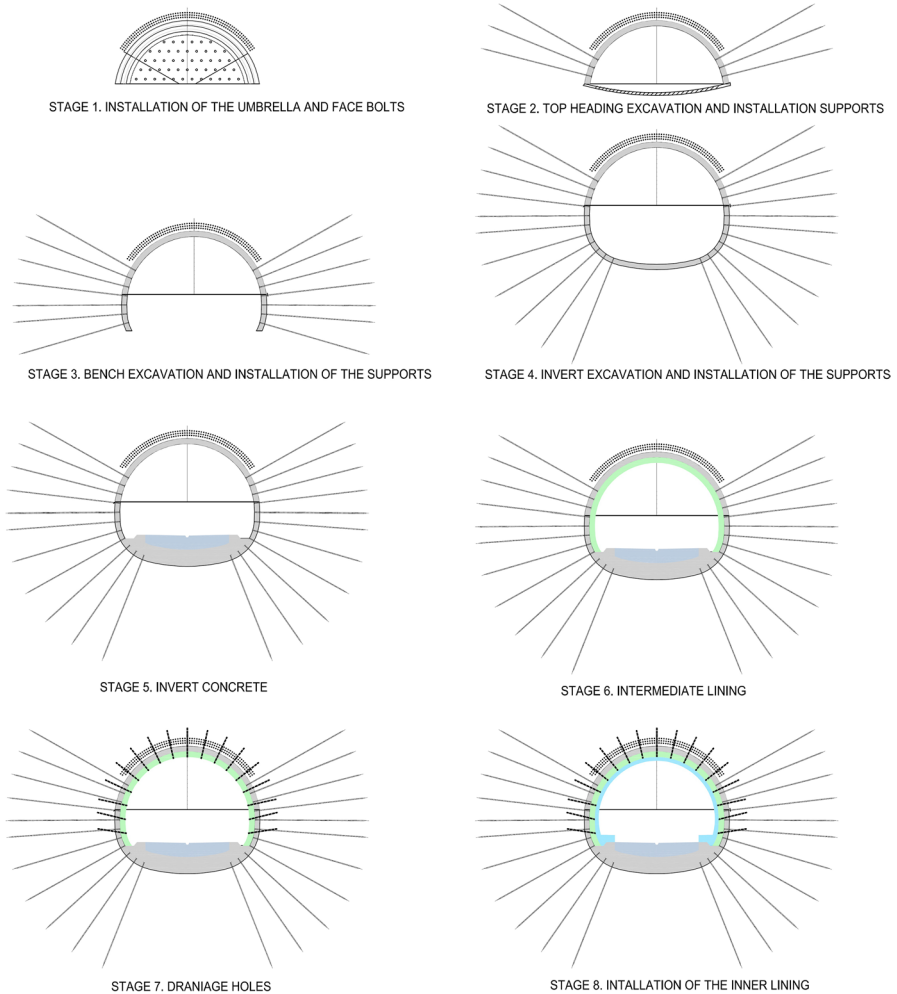
Fig. 11 Excavation stages

in the third stage, bench excavation is performed; and in the fourth stage, invert excavation and supports are completed. In the fifth stage, the excavation process is completed by invert construction. After this stage, the intermediate lining is constructed, and in the next stage, drainage holes are drilled. After all these processes are completed, the tunnel support is completed by the inner lining concrete. All these stages must be performed as soon as possible.

3.3 Preliminary Tunnel Support System Evaluation

In the first stage, analytical solutions are performed for the preliminary assessment of the support system. Equations (Hoek and Brown, 1980; Hoek, 2007 and 2012)

for the analytical solutions (closed-form solution) were summarized by Aygar and Gokceoglu (2021a). In this section, preliminary assessments are carried out on the behavior of the ground and tunnel support systems for cohesionless units and clay.

The analyses were carried out for three sections:

(a) 30 m of overburden height (cohesionless unit)
(b) 60 m of overburden height (clay unit)
(c) 90 m of overburden height (cohesionless unit)

For these units, the field stress, strength σ_{cm}, ratio of the strength to the in situ stress, plastic zone radius, unit strain ($\mathcal{E}$), and deformation in unsupported tunnel calculated equations are given in Table 3 (Hoek and Brown, 1980; Hoek, 2007 and Hoek 2012), and the results are given in Table 4. In Fig. 12, the closure is given for 3 phases, and it is not at an acceptable level; hence, before the excavation, the tunnel face and ceiling should be reinforced with umbrella and face soil nails.

3.4 Rock Support Interaction Analysis—Characteristic Curves

When determining tunnel support systems, it is necessary to determine the ground reaction curve (GRC) and the support system reaction curve (SRC). In addition, it is of particular importance to know the longitudinal deformation profile (LDP) before supporting the tunnel. Such approaches are a decisive criterion, especially in determining the loads on supports. The ground characteristic curve (GRC), support system characteristic curve (SRC), and longitudinal displacement profile (LDP) curve were drawn for these sections of the tunnel. For a 30-m, 60-m, and 90-m overburden, the ground reaction curves, longitudinal displacement profile, and support reaction curves are given in Figs. 13 and 14 using the Vlachopolos and Diederichs (2009) equations.

$$u_0^* = \frac{u_0}{u_{max}} = \frac{1}{3}e^{-0.15R^*}$$

$$
\begin{aligned}
u_0^* &= \frac{u_0}{u_{max}} = \frac{1}{3}e^{-0.15R^*} \\
u^* &= \frac{u}{u_{max}} = u_0^* e^{X*} \text{ for } X* \leq 0 \text{ (in the rock mass)} \\
u^* &= 1 - \left(1 - u_0^*\right)e^{-\frac{3X*}{2R*}} \text{ for } X* \leq 0 \text{ (in the tunnel)}
\end{aligned}
\tag{10}
$$

where $R^* = R_p/R_T$

Equations are given under the condition of hydrostatic field stresses for steel ribs, shotcrete lining, and bolts in a circular tunnel. The summary table of the support system selected in both parts of the tunnel is given in Table 5.

The support pressure, support stiffness, and maximum displacement are given in Table 6 for support types using equations by Hoek and Brown (1980) and Hoek et al. (2008)

Table 3 Closed-form solution equations (Hoek and Brown, [1980](#); Hoek, [2007](#) and Hoek [2012](#))

Mohr–Coulomb criteria (1)	$\sigma_{1'} = \sigma_{cm} + k\sigma_{3'}$	Radius of the plastic zone, r_p when $p_i = 0$ (6)	$r_p = r_0 [(\frac{2(p_0(k-1)+\sigma_{cm})}{(1+k)((k-1)p_i+\sigma_{cm})}]^{\frac{1}{k-1}}$
			$r_p = r_0 [(\frac{2(p_0(k-1)+\sigma_{cm})}{(1+k)((k-1)p_i+\sigma_{cm})}]^{-\frac{1}{k-1}}$

The uniaxial compressive strength of the rock mass, σ_{cm} (2)	$\sigma_{cm} = \frac{2c'\cos\theta}{1-\sin\theta} + k\sigma_{3'}$	Inward radial displacement u_{ip} (7)	$u_{ip} = (\frac{r_0(1+\theta)}{E_m})[2(1-\vartheta)(p_0-p_{cr})(\frac{r_p}{r_0})^2 - (1-2\vartheta)(p_0-p_i)]$
The slope k of the versus $\sigma'_1 - \sigma'_3$ (3)	$k = \frac{1+\sin\theta'}{1-\sin\theta'}$	Percent strain, ε (8)	$\varepsilon(\%) = (\frac{u_i}{r_0}) \times 100 = [0.2 - 0.25(\frac{p_L}{p_0})(\frac{\sigma_{cm}}{p_0})^{2.4(\frac{p_L}{p_0})-2}$
Critical support pressure p_{cr} (4)	$p_{cr} = \frac{2p_0 - \sigma_{cm}}{1+k}$	Radius of the plastic zone (9)	$(\frac{r_p}{r_0}) = (1.25 - 0.625(\frac{p_L}{p_0})(\frac{\sigma_{cm}}{p_0})^{(\frac{p_L}{p_0})-0.57}$
Radial elastic displacement u_{ie} (5)			

$$u_{ie} = \frac{r_0(1+\vartheta)(p_0 - p_i)}{E_m}$$

r_p = radius of plastic zone

u_i = tunnel sidewall deformation

r_0 = original tunnel radius in meters

p_i = internal support pressure

p_0 = in situ stress

E_m = deformation modulus

ϑ = Poisson's ratio

σ_1' = axial stress at which failure occurs

σ_3' = confining stress

c' = cohesion

ϕ' i ϕ' = friction angle of the rock mass

Table 4 Analytical solution results

	σ_{cm}	P_0	σ_{cm}/P_0	r_p (m)	$\mathcal{E}$ (%)	u_i (m)	u_{if} (m)	P_{cr} (MPa)
Cohesionless unit ($h = 30$ m)	0.02	0.63	0.03	30	3.18	0.51	0.09	0.26
Clay ($h = 60$ m)	0.015	1.26	0.118	40	7.87	1.26	0.19	0.74
Cohesionless unit ($h = 90$ m)	0.15	1.89	0.01	46	22	3.5	0.49	0.80

The maximum displacements in the tunnel face reach 50 cm (Table 7). In this case, it has been shown that the tunnel does not have an unsupported stand-up time. Before starting the excavation, it is evident that face nails and umbrellas for the ceiling section are necessary. In addition, as shown in Fig. 13, the supports in the tunnel need to be installed immediately; otherwise, the deformation tends to increase rapidly. In addition, the plastic zone radius is up to 16 m for a 30-m overburden, 30 cm for a 60 -m overburden, and 35 m for a 90-m overburden. Consequently, the tunnel is in a completely plastic zone.
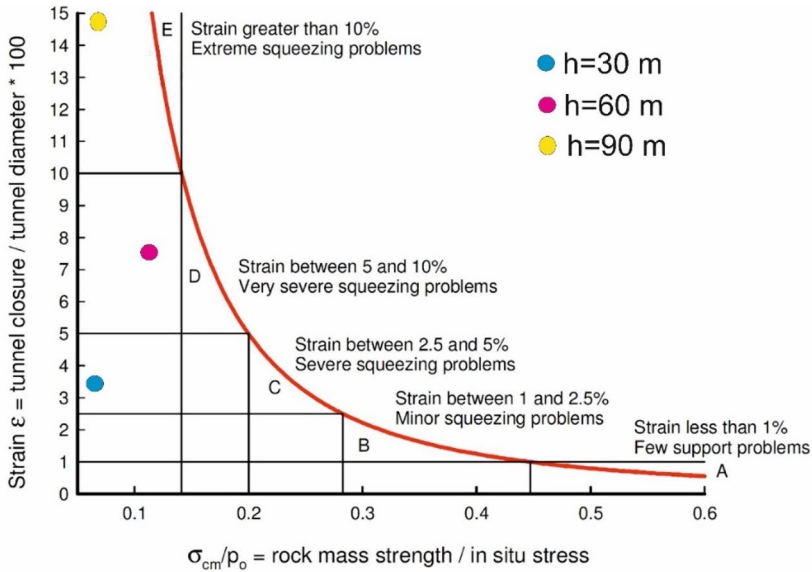
4 3D Numerical Analyses

3D numerical analyses are performed with the FLAC3D v2.10–22 (Itasca, 2002) program. FLAC3D is a numerical analysis program that works with the finite difference method and enables the monitoring of mechanisms such as plastic flow and collapse with the Lagrange computation scheme and mixed discretization technique (Khanbabazadeh and Iyisan 2014). Since matrix elements are not used in FLAC3D software, they do not occupy substantial computer memory, so large-scale models can be analyzed. It is possible to model the ground exactly with the FLAC3D program, and it is also possible to model the structural elements (bolt, shotcrete, steel ribs, anchor) (Itasca, 2002).

4.1 Model Settings

The models created for the analyses are given in Fig. 15. First, analyses are performed for cases where there were no umbrella or face nails. In the model, a vertical plane of symmetry conditions is used, so half of the tunnel is selected for analyses.

The model was determined to be 100 m in the Y-direction, 100 m in the Z-direction, and 70 m in the X-direction (Fig. 15). The gravity method is used in the analysis, and the Mohr–Coulomb criterion is chosen as the failure criterion. In the analysis, the excavation phases are planned in the top heading, bench and invert, and the boundary conditions are given in Fig. 16. The model is fixed at 0 and 100 points in the y-direction, − 70 points in the z-direction, and 0 and 70 points in the x-direction. In the model, 142,100 zones and 149,253 node points are used. In the model, the mesh spacing around the tunnel is taken as 1.0 m for detailed investigation. Larger mesh intervals are preferred from the tunnel periphery to the surface. Thus, the

	Strain ε %	Geotechnical issues	Support types
A	Less than 1	Few stability problems and very simple tunnel support design methods can be used. Tunnel support recommendations based upon rock mass classifications provide an adequate basis for design.	Very simple tunnelling conditions, with rockbolts and shotcrete typically used for support.
B	1 to 2.5	Convergence confinement methods are used to predict the formation of a 'plastic' zone in the rock mass surrounding a tunnel and of the interaction between the progressive development of this zone and different types of support.	Minor squeezing problems which are generally dealt with by rockbolts and shotcrete; sometimes with light steel sets or lattice girders are added for additional security.
C	2.5 to 5	Two-dimensional finite element analysis, incorporating support elements and excavation sequence, are normally used for this type of problem. Face stability is generally not a major problem.	Severe squeezing problems requiring rapid installation of support and careful control of construction quality. Heavy steel sets embedded in shotcrete are generally required.
D	5 to 10	The design of the tunnel is dominated by face stability issues and, while two-dimensional finite analyses are generally carried out, some estimates of the effects of forepoling and face reinforcement are required.	Very severe squeezing and face stability problems. Forepoling and face reinforcement with steel sets embedded in shotcrete are usually necessary.
E	More than 10	Severe face instability as well as squeezing of the tunnel make this an extremely difficult three-dimensional problem for which no effective design methods are currently available. Most solutions are based on experience.	Extreme squeezing problems. Forepoling and face reinforcement are usually applied and yielding support may be required in extreme cases.

Fig. 12 Approximate relationship between the strain and the degree of difficulty associated with tunneling through squeezing rock. Note that this curve is for tunnels with no support (Hoek and Marinos, 2000)
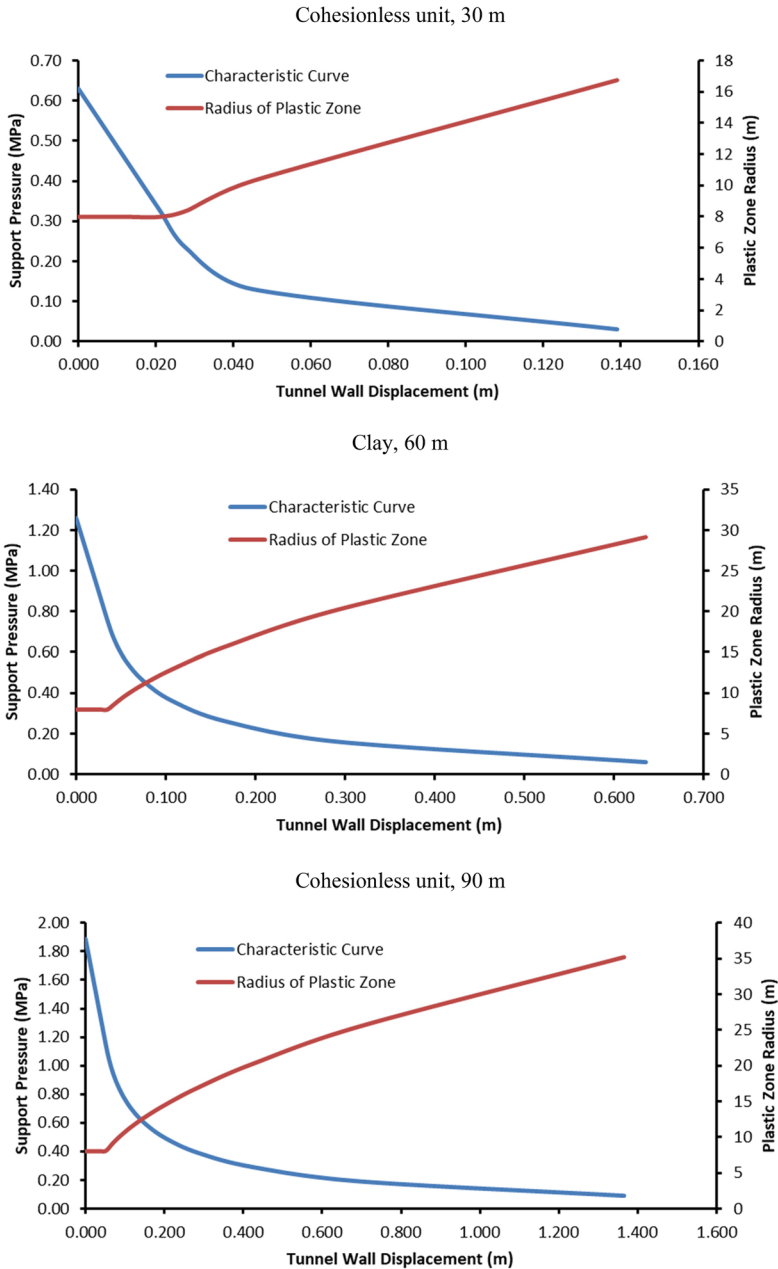
Cohesionless unit, 30 m

Clay, 60 m

Cohesionless unit, 90 m

Fig. 13 Characteristic curves for different overburdens and units

solution time is shortened. In the model, a cylindrical shell and radcylindrical mesh type are used.

For the numerical analyses, the bulk modulus and shear modulus are necessary, and the parameters used in the analyses are given in Table 8. These values are

related to the Poisson ratio (v) and modulus of deformation (E). These equations for the bulk modulus and shear modulus are described by Eqs. 17 and 18.

Bulk modulus

$$K = E/(3 * (1 - 2 * v))$$ (17)

Shear modulus

$$G = E/(2 * (1 + v))$$ (18)

In the analyses, the excavation stage is chosen as 1.0 m in the top heading, 2 m in the bench, and 4 m in the invert. To establish the initial excavation conditions in the model, it is assumed that the excavation and supports of the 60-m section in the top heading and the 36-m section in the bench and the invert are completed. Additionally, the outer lining is completed. Modeling stages are given in Table 9.

Shotcrete is defined as a shell element in the model, and intermediate lining (Fig. 17) is defined as a block (Table 10).

For rock bolt modeling in the tunnel, the ground parameters (cohesion and modulus of deformation) are increased, and the strength parameters of the material around the tunnel are defined as composite material (Table 11). Consequently, ground and rock bolts are defined as a single unit. Around the tunnel, 88.9-mm diameter self-drilling injection pipe-driving elements are used as bolts. The main reason for this preference is because the ground is not cohesive or has low cohesion. This is because bolt drills opened with low drilling diameters on such soils are closed immediately, and the injection cannot go around the tunnel. For this reason, the bolt diameter and drill diameter are chosen to be large.

4.2 Static Analysis Results for the 3 Cases

During the first stage, analyses are performed without umbrella and soil nails, and the stability of the tunnel face is investigated. The importance of face stability in cohesionless soils is emphasized. In addition, the effect of the tunnel stability on the deformations of the face soil nails, and the umbrella and the tunnel stability effect are also investigated. The results are evaluated for 3 different overburden sections. For the 30-m overburden, a 20-cm deformation (Fig. 17a) occurred in the Y-direction, that is, in the tunnel face, towards the inside of the tunnel in cohesionless units. A 65-cm (Fig. 17b) deformation (in total) occurs in the Z-direction (the vertical direction). In the analyses for clayey units ($h = 60$ m), a total vertical deformation of up to 5 cm and a displacement of up to 8 cm in the tunnel face are observed (Figs. 18a and b). For the 90-m overburden height, vertical deformation of up to 8 cm and deformation of up to 16 cm in the Y-direction (tunnel face) occurs (Fig. 19a and b). The results are presented in Table 12.

Deformations in the tunnel face continue upwards in sandy units due to the cohesionless character. In clayey units, deformations are concentrated only in the center of the tunnel face due to the cohesive nature of the ground.
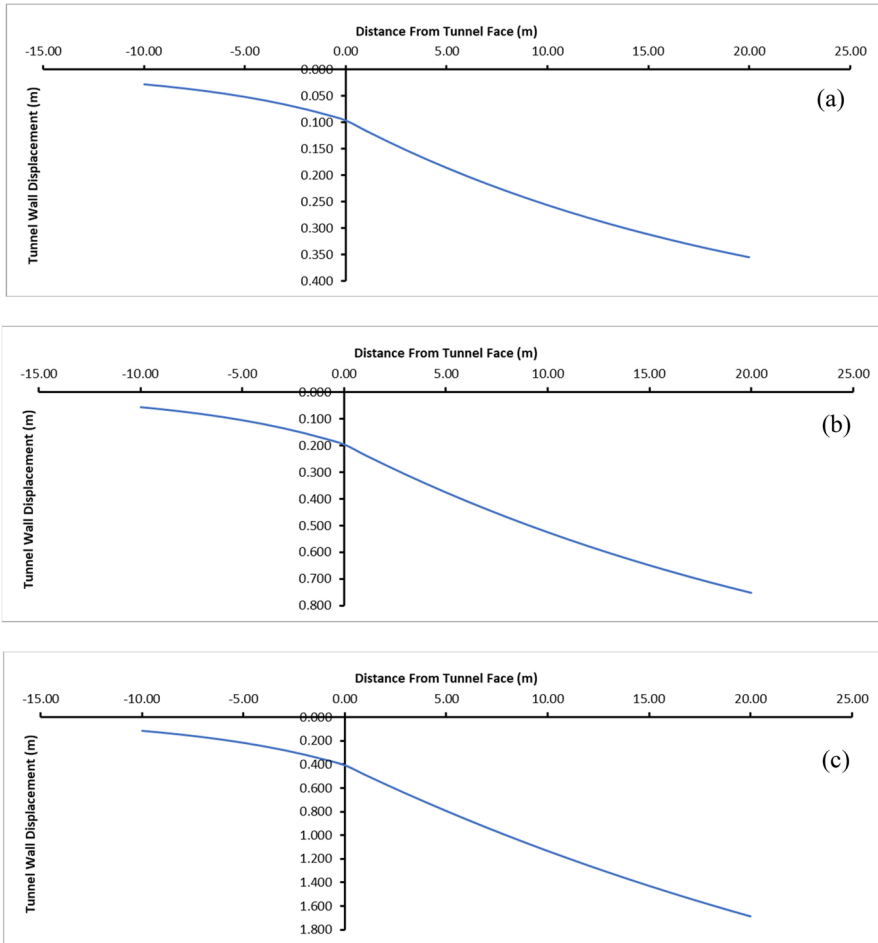
Fig. 14 Longitudinal deformation profiles for different overburdens and units: **a** cohesionless unit, 30 m; **b** clay, 60 m; and **c** cohesionless unit, 90 m

To ensure the stability of the tunnel face, before starting the excavation on the tunnel face and tunnel ceiling, cable bolts and umbrellas should definitely be inserted. The parameters of the cable bolts and umbrellas used in the analyses are given in Tables 13 and 14. The umbrella system is defined as a pile element in the FLAC3D program. This definition is also referenced by Oke et al. (2012, 2013a and Oke et al., 2013b, Oke et al., 2014a and Oke et al. 2014b). The cable bolts and umbrella system used in the model are given in Fig. 20.

The cable bolts and umbrellas used in the model are selected as 12 m. Cable bolts are applied to the model at 1.0×1.0 m intervals and a 6-m overlap. Umbrellas are also defined in the model with an overlap of 6 m, and they are applied in 3 rows due to the variable height of the cover and the non-cohesion/low cohesion of the ground.

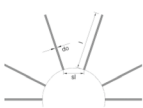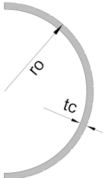**Table 5** Support capacity equations (Hoek and Brown 1980; Hoek et al. 2008)

Steel Set		
	σ_{ys} is the yield strength of the steel (MPa) E_s is the Young modulus of the steel (MPa) A_s is the cross-sectional area of the section (m²) s_l is the set spacing along the tunnel axis (m) r_o is the radius of the tunnel (m) P_{ssmax} is the maximum support pressure K_{ss} is the stiffness	$Pssmax = \frac{As*\sigma ys}{sl*lro}$ (11) $Kssmax = \frac{Es*As}{sl*lro^2}$ (12)

Rock Bolts		
	d_b is the rockbolt or cable diameter (m) l is the free length of the bolt or cable (m) E_s is the Young modulus of the bolt or cable (MPa) s_c is the circumferential bolt spacing (m) s_l is the longitudinal bolt spacing (m) T_{bf} is the ultimate bolt or cable load P_{sbmax} is the maximum support pressure K_{ss} is the stiffness	$Psbmax = \frac{Tbf}{sl*sc}$ (13) $Ksb = Es*\pi*\frac{db^2}{4lslsc}$ (14)

Concrete or Shotcrete		
	σ_{cc} is the uniaxial compressive of the concrete or shotcrete (MPa) E_c is the Young modulus of the concrete or shotcrete (MPa) υ is the Poisson ratio of the concrete or shotcrete t_c is the thickness of the lining (m) r_o is the radius of the tunnel (m) P_{scmax} is the maximum support pressure K_{ss} is the stiffness	$Pscmax = \frac{\sigma cc}{s}*\left[1-\frac{(ro-tc)^2}{ro^2}\right]$ (15) $Ksc = \left(Ec*\frac{ro^2-(r0-tc)^2}{2*(1-\vartheta^2)*(r0-tc)*ro^2}\right)$ (16)

Table 6 Support system pressures

	p_{scmax}(MPa)	K_{sc} (MPa/m)	u_{icmax}(m)
Shotcrete (ds = 50 cm)	1.51	254.38	0.106
Steel rib (I 300)	0.419	29.75	0.114
Rock bolts	0.373	190.78	0.102

Table 7 Displacements in the tunnel face

	r_{pm}/r_0	Tunnel face displacement u_{if} (m)	Tunnel face displacement u_{if} (1 m behind the face) (m)	Maximum displacement u_{im} (m)	Face displacement/max displacement u_{if}/u_{im}
Cohesionless unit, $h = 30$ m	3.87	0.096	0.12	0.51	0.180
Clay, $h = 60$ m	5.07	0.190	0.235	1.25	0.155
Cohesionless unit, $h = 90$ m	6.93	0.400	0.49	2.60	0.117

Analyses for 30-m, 60-m, and 90-m overburdens are given in Fig. 21, and the displacements in the *Y*- and *Z*-directions can be followed here. With these supports, the deformations in the *Z*-direction after excavation in cohesionless units ($h = 30$ m) of the tunnel ceiling decrease to 10 cm, and the deformations in the *Y*-direction
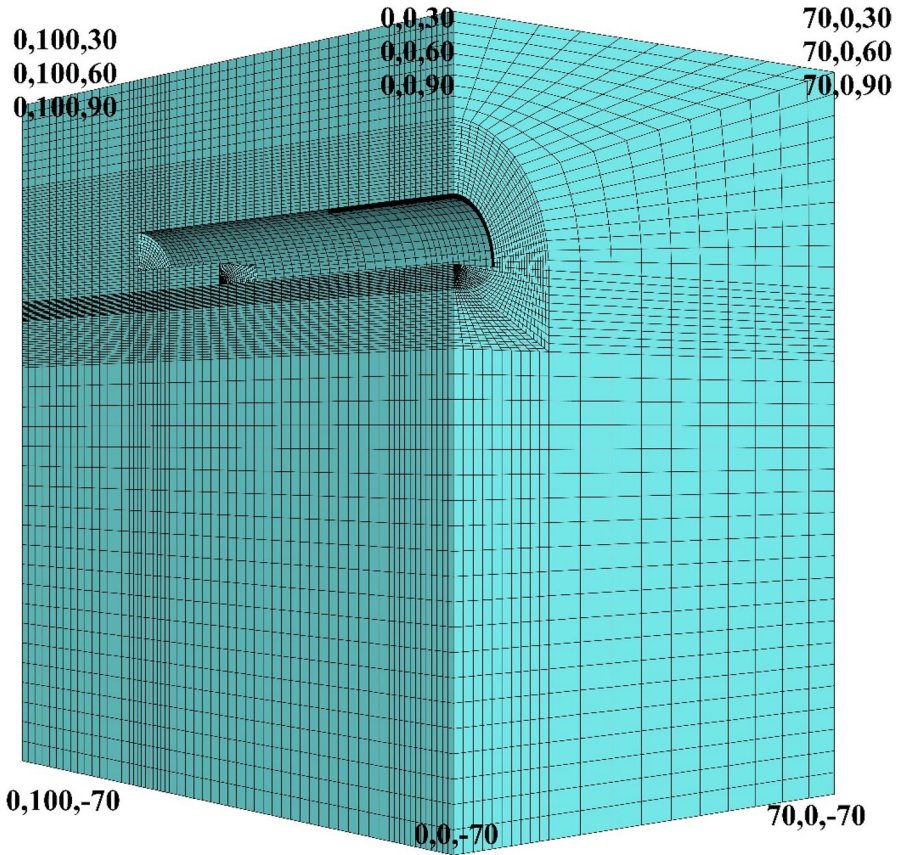
Fig. 15 FLAC3D model for different tunnel sections (cohesionless unit, 30 m; clay, 60 m; and cohesionless unit, 90 m)

decreased to 2.75 cm. In clay units ($h = 60$ m), the deformations in the Y-direction in the tunnel decrease to 5 cm after the application of umbrella and cable bolts. Under the 90-m overburden, the deformations decrease to 8 cm in the Y-direction and 7 cm in the Z-direction. The results are given in Table 15.

As can be seen from the analysis results, the face support has a significant effect on the tunnel stability. Vertical deformations exceeding 60 cm without face supports decrease to 10 cm with face supports, and deformation decreases from 20 to 2.5 cm in the tunnel face.

The deformations obtained from the analytical solutions in the tunnel face are given in 7). For the 30-m overburden, the deformation is 20 cm; for the 60-m overburden, the deformation is 20 cm; and for the 90 m overburden, the deformation is 40 cm. In the numerical analysis, the deformations in the tunnel face towards the inside of the tunnel are 20 cm at 30 m at overburden height, 8 cm at a 60-m overburden height, and 16 cm at under 90 m of overburden height (Table 12). In the numerical analysis, the deformations in the cohesionless unit
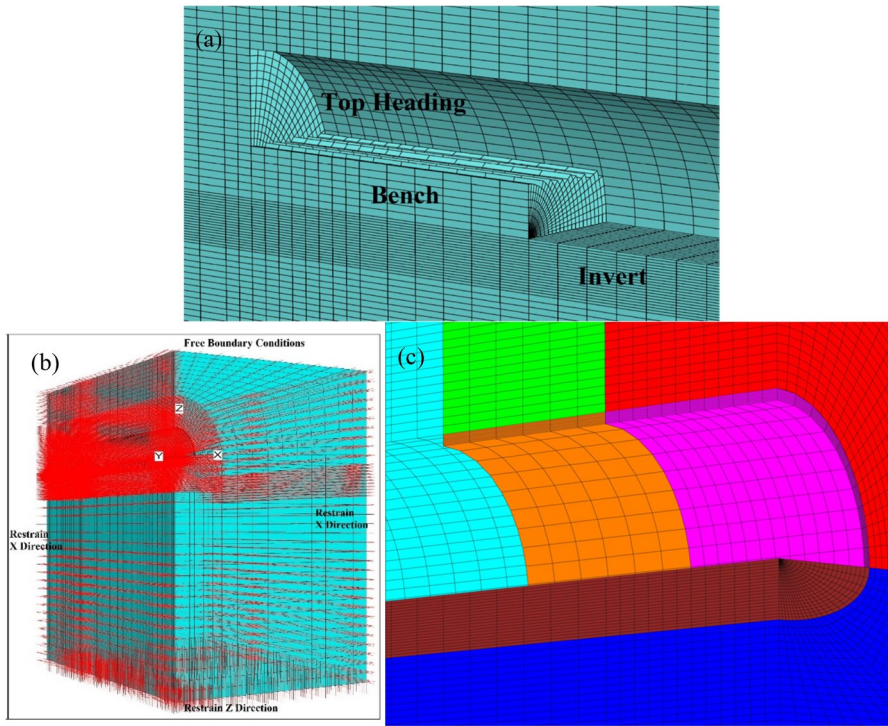
Fig. 16 Planned excavation steps: **a** model boundary conditions, **b** excavation, and **c** intermediate lining

Table 8 Bulk, shear, and deformation modulus

Unit	E (deformation modulus, MPa)	υ (Poisson ratio)	K (bulk modulus, MPa)	G (shear modulus, MPa)
Cohesionless unit	150	0.3	125	58
Clay	200	0.3	167	77

are lower than the analytical solutions. The main reason here is that the upper half of the excavation height is low due to the partial excavation of the tunnel. However, analytical solutions are performed for full face excavation.

5 Seismic Analysis of Tunnel Support Systems

The behavior of underground structures during earthquakes is different from that of surface structures. Because underground structures are surrounded by the ground, they are less affected by earthquakes than surface structures (Hashash

Table 9 Modeling stages

Stage	Explanation	Stage	Explanation
1	Unbalanced forces	10	Excavation between 63 and 64 m in TH
2	Excavation and support installation between 0–60 m full face excavation and 40–60 m bench excavation and invert excavation 0–36 m invert Sect. 0–12 m intermediate lining installation	11	Excavation between 44 and 46 m in bench
3	Reset the displacements Excavation between 60 and 61 m in TH	12	Excavation between 64 and 65 m in TH
4	Excavation between 61 and 62 m in TH	13	Excavation between 65 and 66 m in bench
5	Excavation between 40 and 42 m in bench	14	Excavation between 46 and 48 m in bench
6	Excavation between 42 and 44 m in bench	15	Excavation between 40 and 44 m in invert
7	Excavation between 36 ad 40 m in invert	16	Excavation between 66 and 67 m in TH
8	Installation of the intermediate lining between 12 and 24 m	17	Excavation between 67 and 68 m in TH
9	Excavation between 62 and 63 m in TH	18	Seismic analysis

et al., 2001). However, it was observed that the earthquakes such as Japan, Taiwan, and Turkey that occurred after the 1990s in the world caused severe damage to the underground structures (Hashash et al., 2001). For this reason, ground failure effects such as fault slip, liquefaction, and slope stability problems are important during the selection of tunnel routes and the locations of underground structures. However, due to the strict geometrical constraints of high-speed railways, it is not always possible to avoid adverse geological-geotechnical conditions.

Sakurai and Takahashi (1969), Owen and Scholl (1981), O'Rourke (1984), Wang (1993), O'Rourke et al. (2001), and Penzien (2000) studied the seismic design of underground structures. In these studies, the methods used in the design of the tunnel lining are explained in detail. The tunnel is located in the seismically active NAFZ, and hence, the support stability was checked under seismic conditions. According to the extremely weak units and within the North Anatolian Fault Zone, one of the most active fault zones in the world, tunnel stability is also very important. Hence, it is also possible to perform dynamic analysis with the FLAC3D program. A fully nonlinear analysis method is used in the FLAC3D program, and it can model the problem more accurately (Itasca 2002; Khanbabazadeh and Isiyan, 2014). There are 3 main parts to be considered when performing dynamic analyses via the FLAC3D program (Itasca, 2002).

a) Application of dynamic loading and boundary conditions
b) Ensuring that the wave is properly analysed
c) Mechanical damping

The viscous boundary conditions (quiet boundary) were chosen as the boundary conditions to be used in the model. Quiet boundary conditions, proposed by
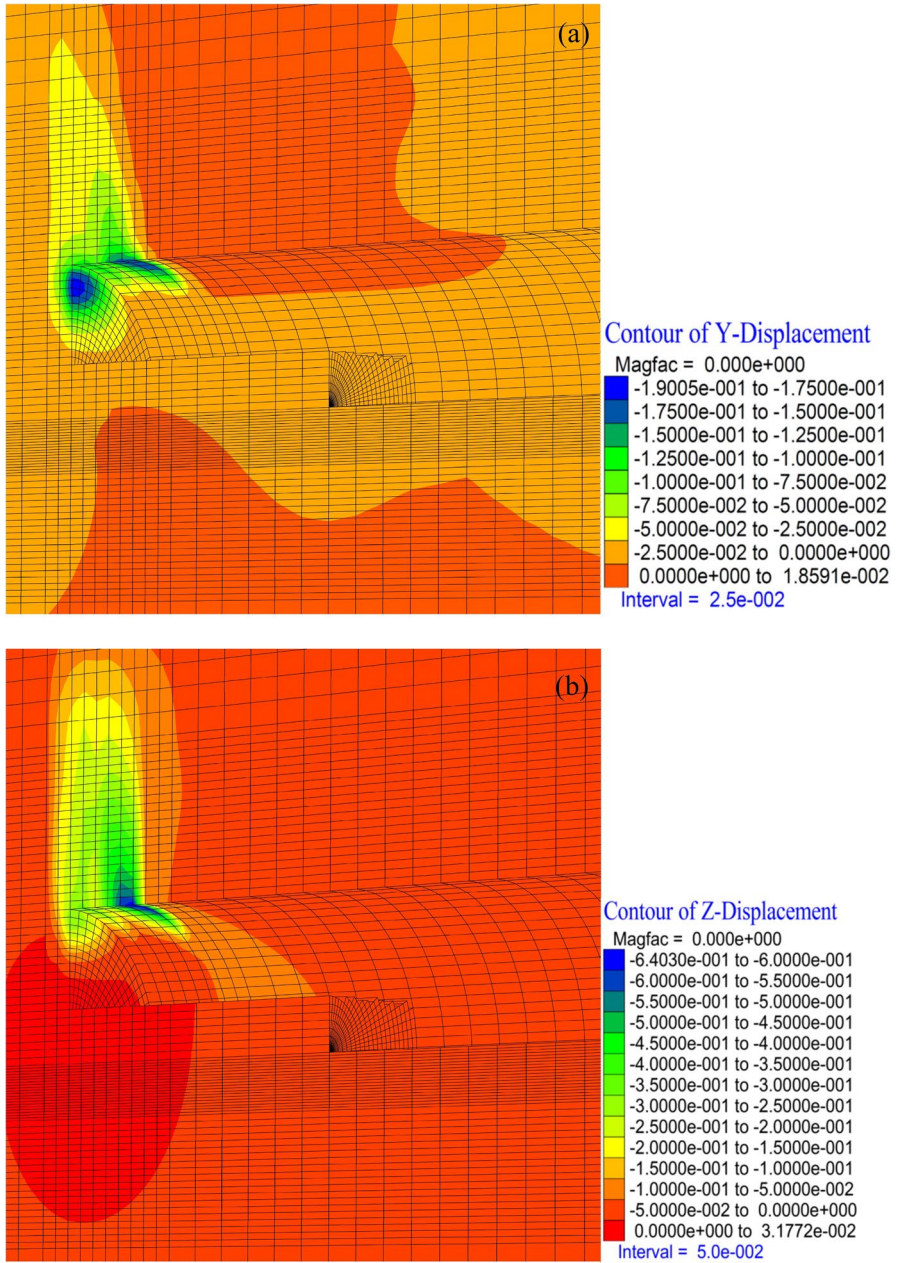
Fig. 17 Displacements occurring in the *Y–Z*-direction (*h* = 30 m, cohesionless unit): **a** displacements in the *Y*-direction and **b** displacements in the *Z*-direction

Table 10 Strength parameters used for shotcrete and intermediate lining concrete

Element	E_i (GPa)	$\sqrt{}$	Υ (kg/m³)
Shotcrete	20	0.25	2500
Intermediate lining	35	0.25	2500

Table 11 Ground parameters for units reinforced with rock bolts

Bolt drilling diameter	0.089
Distance between two bolts	1.00 m
q_u (uniaxial compressive strength)	1.0 MPa
a_r (area ratio)	0.00453416
E_{soil} (soil deformation modulus)	80,000 kPa
ϕ_{soil} (soil internal friction angle)	35°
c_{soil} (soil cohesion)	5 kPa
c_{in} (cohesion of injection)	10.0 MPa
E_{in} (Young modulus of injection)	1,000,000 kPa
c_{comp} (cohesion of composite material)	50 kPa
ϕ_{comp} (internal friction angle of composite material)	0°
E_{comp} (Young modulus of composite material)	84,171 kPa

Lysmer and Kuhlemeyer (1969), prevent the wave applied to the model from being reflected from the boundary. The frequency of the wave to be applied to the model, the characteristics of the wave, and the wavelength are critical for the accuracy of the analysis (Khanbabazadeh, and Iyisan, 2014; Itasca 2002). Here, the largest mesh spacing used in the numerical model should be one-tenth of the wave size or smaller (Itasca, 2002).

$$\Delta l \leq \frac{\lambda}{10} \tag{19}$$

Δl mesh spacing
Λ wavelength

$$f = \frac{C}{\lambda} \tag{20}$$

F wave frequency
The frequency to be calculated based on the largest mesh range in the model is determined.

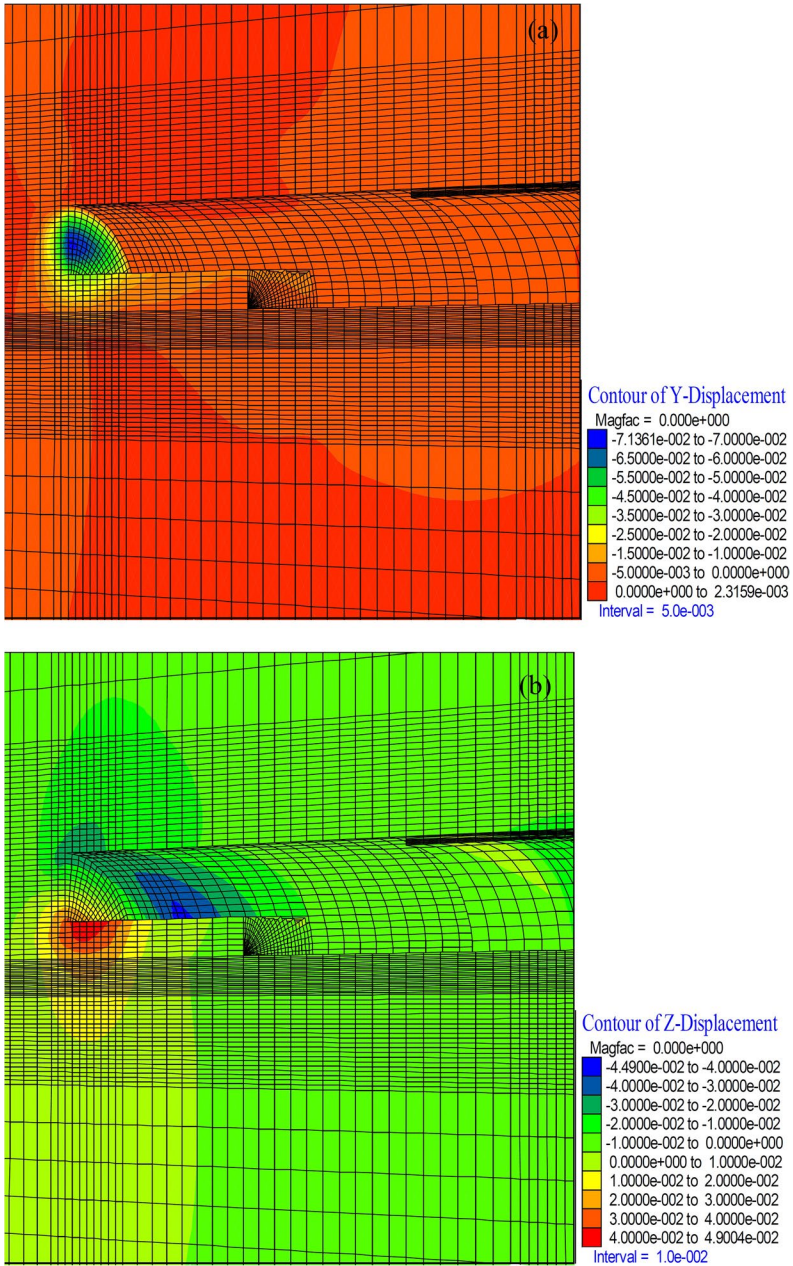$$f = \frac{Cs}{10 * \Delta l} \tag{21}$$

f frequency
Cs shear wave velocity

Fig. 18 Displacements occurring in the *Y–Z*-direction (*h* = 60 m, clay unit): **a** displacements in the *Y*-direction and **b** displacements in the *Z*-direction

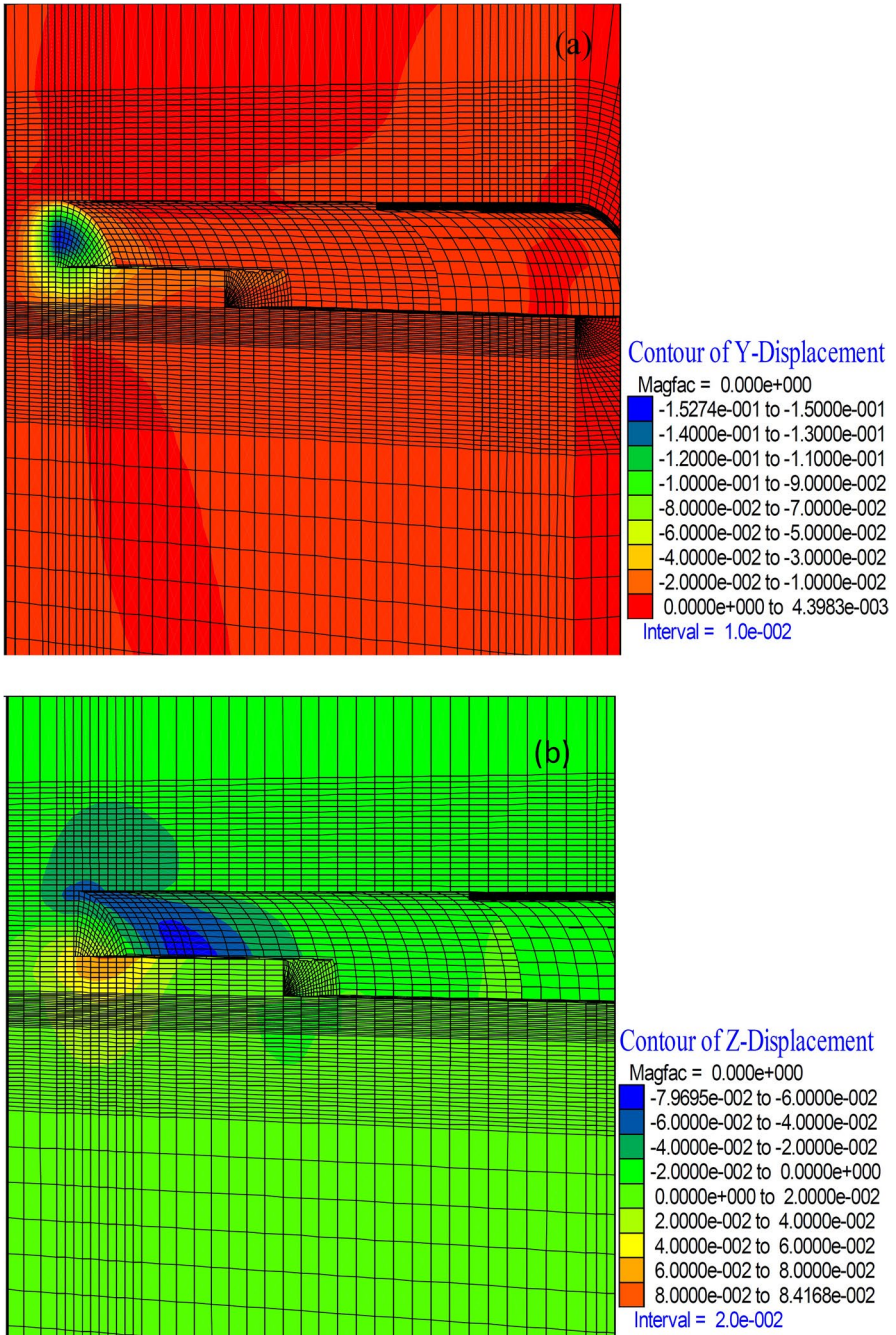$$Cs = \sqrt{G/\rho} \qquad (22)$$

Gshear modulus

Fig. 19 Displacements occurring in the *Y–Z*-direction (*h* = 90 m, cohesionless unit): **a** displacements in the *Y*-direction and **b** displacements in the *Z*-direction

Table 12 Numerical analysis results in the static case without face bolts and umbrella

Overburden (h) m	Vertical deformation (Z-axis) cm	Face deformation (Y-axis) cm
30	65	20
60	5	8
90	8	16

ρ unit weight

The model is given in Fig. 22 and represents the dimensions. This model is only for the 30-m overburden, and analyses were performed for the 30-m, 60-m, and 90-m overburdens. The mesh is defined in the FLAC3D model with 280,600 zones, 287,122 grip points, and 2542 nodes. The model geometry includes x-, y-, and z-axes, in which the y-axis is along the tunnel excavation line, the x-axis is along the transverse direction and the z-axis is in the vertical direction. The x-dimensions are $x = 140$ m, $y = 90$ m, and $z = 30$ m (60 m and 90 m).

The largest mesh spacing used in the model is 5.5 m, and the frequency is calculated to be 1.0 Hz with the help of equations. In the model, the overburden is taken as 60 m and 90 m, and the model is determined to be 140 m in the *X*-direction, 100 m in the *Y*-direction, and 100 m in the *Z*-direction (Fig. 22). The tunnel width is 13 m, and the height is 8.4 m. In the model, the short-term undrained parameters are chosen by considering the soil parameters as short-term parameters at the time of the earthquake.

Seismic loading is applied to the model as a harmonic sine wave for 2.0 s. The applied horizontal acceleration value given by the Disaster and Emergency Management Presidency of Turkey was 0.342 g. The frequency of the wave to be used in the model is chosen as 1.0 Hz, and 5% is taken as Rayleigh damping. The wave base is applied to the model. Since the earthquake performance is evaluated in the long term, the shotcrete and bolts added to the model in the static state are removed, and only the inner lining is entered into the model with an intermediate lining. The intermediate lining is entered into the model as a "shell" element, and the inner lining concrete is defined as the "material."

The results obtained from dynamic analyses are given in this section. In the results of the analysis, the moments and axial forces occurring in the lining are investigated. For a 30-m overburden thickness, the model fails because the ground is completely cohesive. It is observed that the ground undergoes major deformations and that the deformations continue with the displacements in this section. The variation in displacements in the *Z*-direction given in Fig. 23 is given depending on the step. As shown in Fig. 25, the displacements increase linearly.

The bending moments and axial force occurring in the intermediate lining under 60 m of overburden thickness are also given in Figs. 24 and 25, respectively. The moment is determined to be 2.78×10^6 Nm, and the axial force value is determined to be 5.78×10^6 N. In the section investigated, it is revealed that only the intermediate lining could not sufficient and should be considered a bearing element together with the inner lining. In addition, it is known that the thickess of the intermediate

Table 13 Parameters used for cable bolts

Cable modulus (GPa)	Cable modulus (m²)	Cable ultimate tensile capacity (kN)	Grout bond stiffness (N/m/m)	Grout cohesive strength (N/m)
45	1.57×10^{-3}	250	1.75×10^{7}	2.0×10^{5}

Table 14 Parameters used for umbrellas

Diameter of the pipe (m)	Thickness of the pipe (m)	v	E (GPa)	Yield (N)
0.114	0.0065	0.3	200	200000

lining was variable during the application phase. Here, it is thought that the thickness of the intermediate lining is between a minimum of 60 cm and a maximum of 120 cm, and an average lining thickness of 90 cm is considered. When considering the section effects, it is seen that the moment bearing capacity is sufficient with the Intermediate lining (Fig. 26).

The cross-sectional effects determined in the analyses performed under an overburden thickness of 90 m, bending moments calculated to be 3.09×10^{6} Nm (Fig. 27), and the axial force value is estimated to be 5.04×10^{6} N (Fig. 28). In the analyses performed according to the section effects, it is determined that the intermediate lining governs the section effects (Fig. 29).
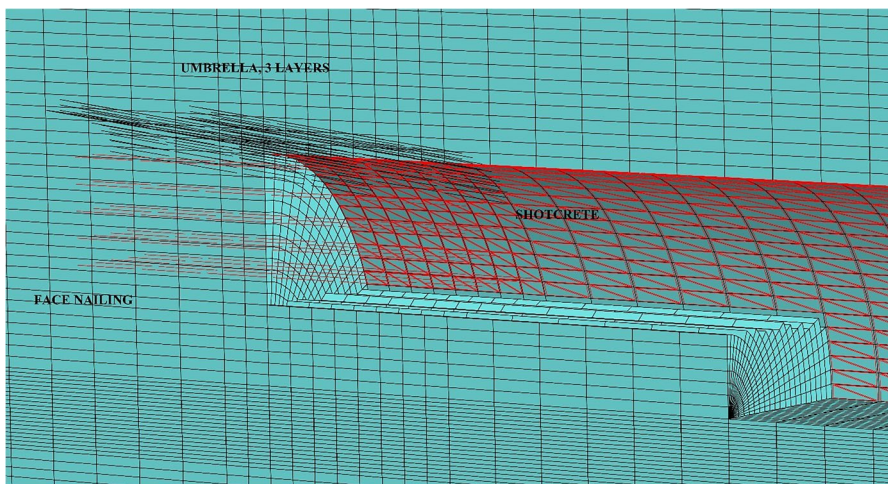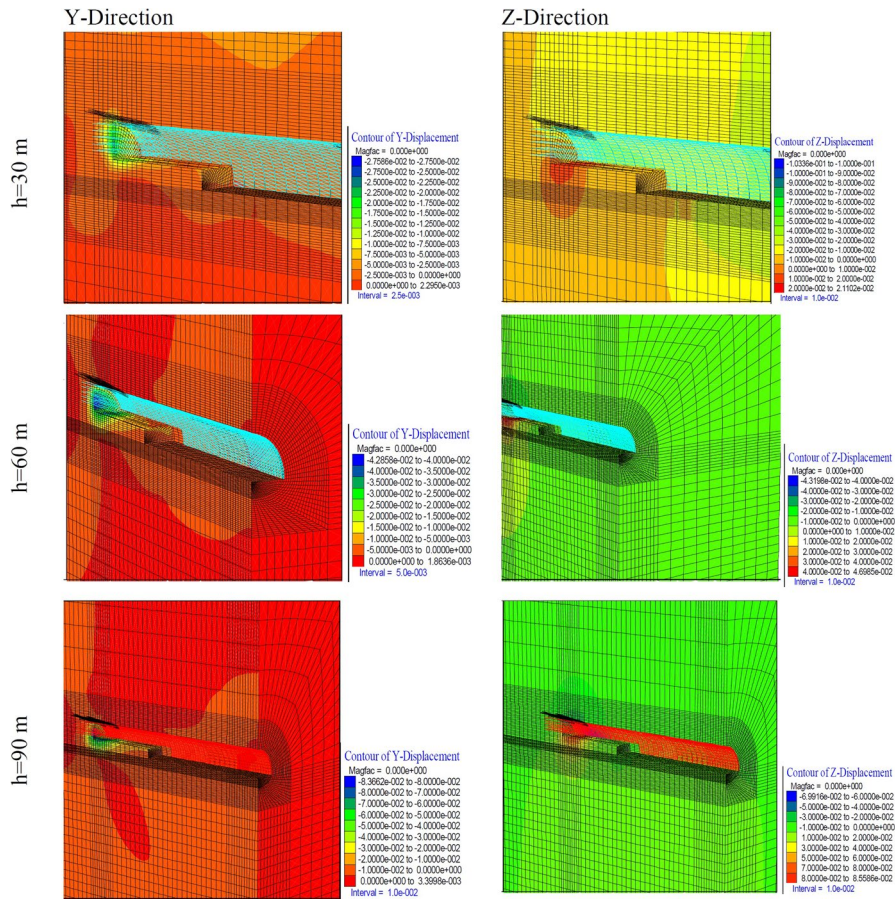

Fig. 20 Support details used in the model

Y-Direction   Z-Direction

Fig. 21 Displacements occurring in the *Y*-direction and *Z*-direction

6 Application and In Situ Measurements

In the tunnel under construction within the scope of the Doğançay project, the intermediate lining is constructed from an average of 40 m behind the tunnel face. Photos

Table 15 Numerical analysis results in face bolts and umbrella systems

Overburden (h) m	Vertical deformation (Z-axis) cm	Face deformations (Y-axis) cm
30	10	2.75
60	3	5
90	7	8
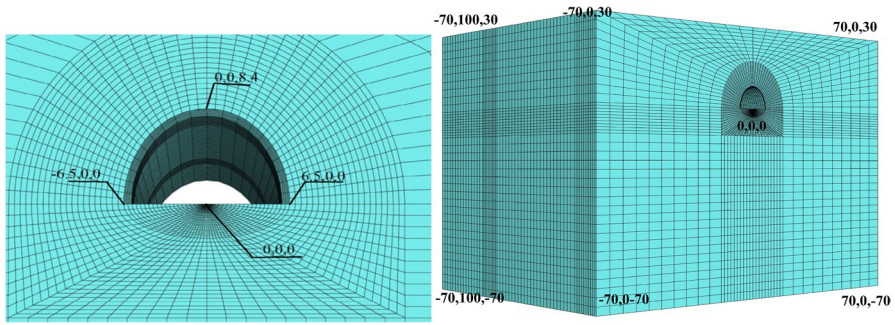
Fig. 22 Model dimensions

from the application stage are given in Fig. 30. The tunnel construction now continues successfully.

The deformations measured at the 5 points in the tunnel section are presented in Fig. 31.

The deformation measurements performed before the intermediate lining are presented in Fig. 32. The deformations are stabilized at nearly 10 cm in the FLAC3D analysis given in Fig. 21. The deformations measured in situ are compatible with the numerical analysis; that is, the vertical deformations are less than 10 cm for the
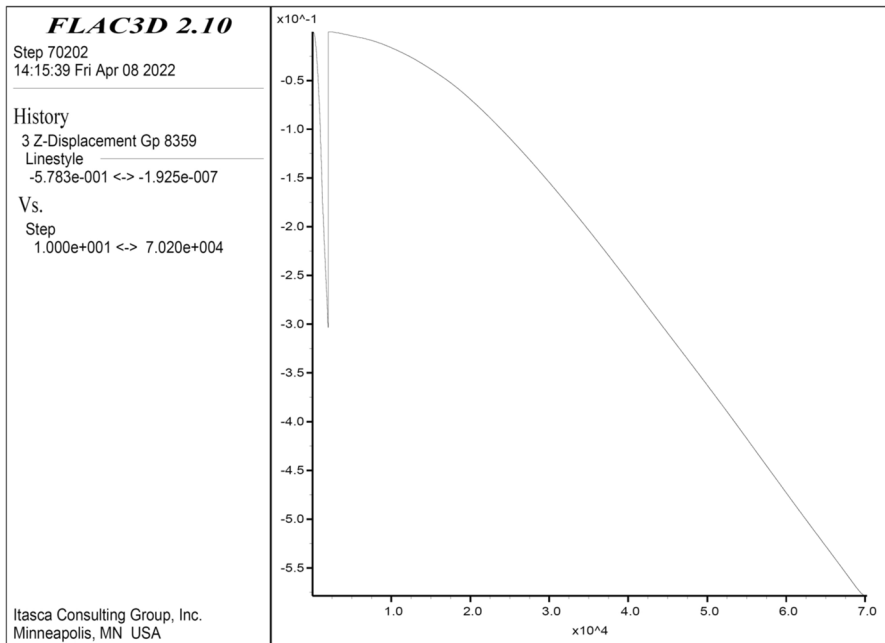
Fig. 23 Vertical displacement for $h = 30$ m
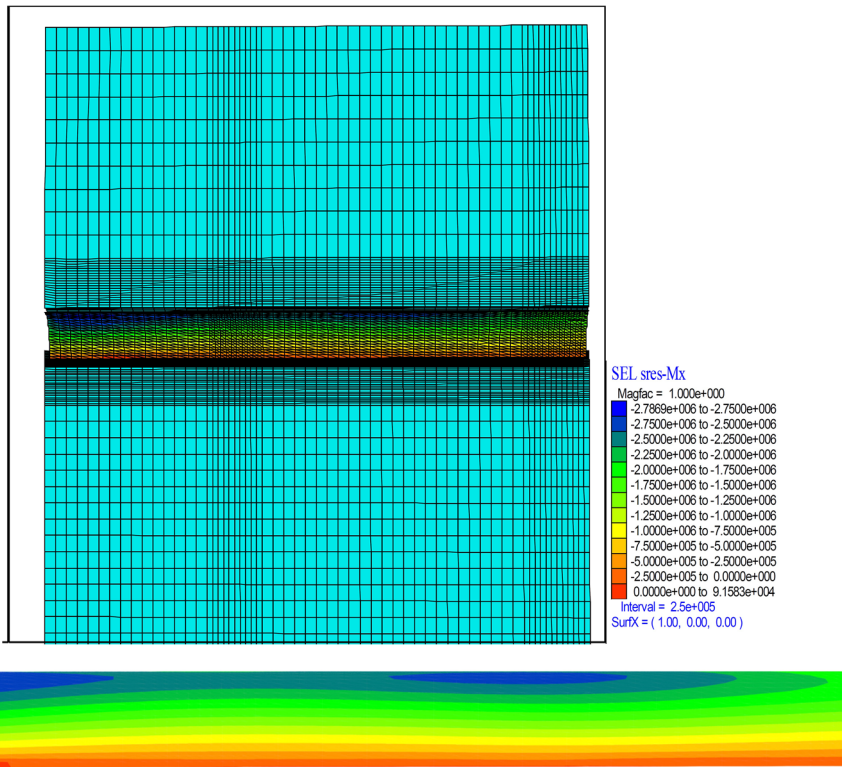
Fig. 24 Bending moments for $h = 60$ m

30-m overburden. The deformation observed in the tunnel is nearly 14 cm in the cohesionless soil.

Additionally, the deformations were measured in the tunnel after intermediate lining application and are given in Fig. 33. As shown in Fig. 33, the deformations are obtained to be less than 1 cm, and stabilization along the tunnel is provided.

7 Conclusions and Recommendations

The T1 tunnel constructed within the scope of the Dogancay project is excavated completely under weak or extremely weak ground conditions. Considering the geotechnical and geological conditions of the tunnel route, the T1 tunnel can be accepted as an interesting case for the tunneling community. However, in the present study, the most critical cohesionless soil and clay sections are investigated with not only analytical solutions but also 3D numerical analyses.

The results of the analyses show that the largest problems encountered in cohesionless soils are face and ceiling stabilization. It is impossible to excavate the
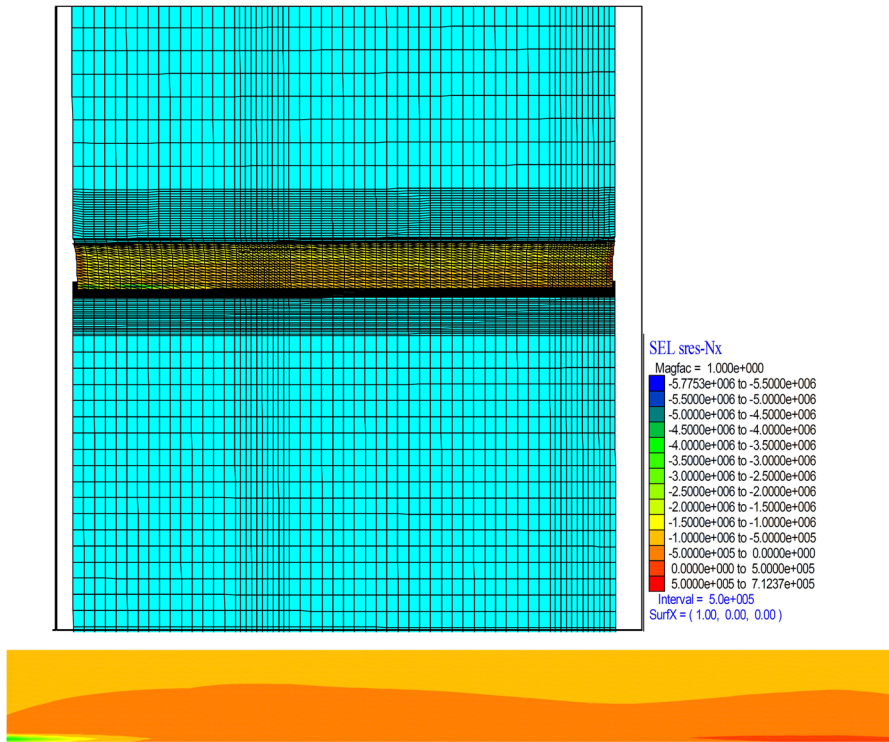
Fig. 25 Axial forces for $h = 60$ m

tunnel without providing ceiling and face stability. To perform consolidation grouting around the tunnel and to ensure arching, in cohesionless soils, the drill diameter should be as large as possible, and accordingly, the diameter of the bolt should be sizeable. With self-drilling bolts, the interaction of water with the clayey ground is minimized. The water comes into contact with the ground at the drill head only and then emerges through the casing. Thus, the tunnel environment is completely improved. In addition, it is necessary to use long and large diameter face bolts and umbrellas to ensure face stability in cohesionless soils. The possible failures in
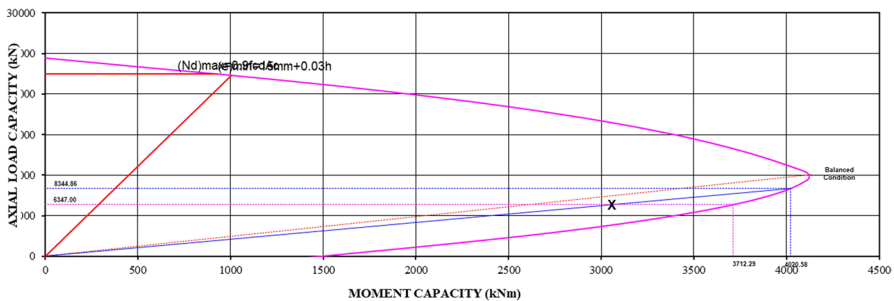

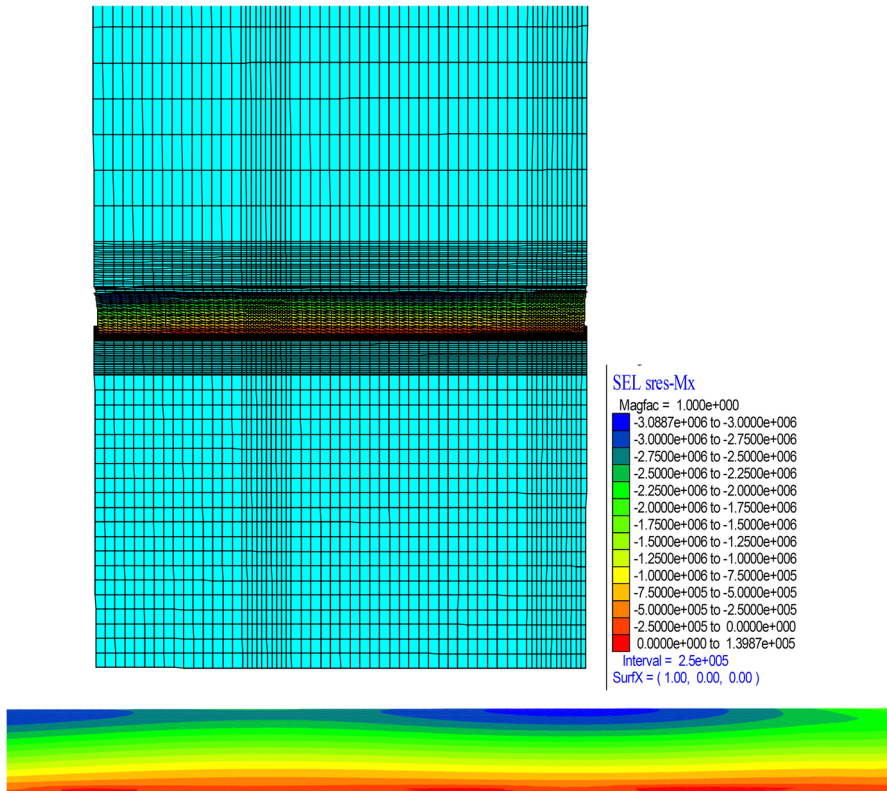**Fig. 26** Interaction diagram in the X-direction for the 60 m overburden

Fig. 27 Bending moments for $h = 90$ m

the tunnel ceiling result in severe problems, and it is appropriate to make a 3-layer umbrella in the ceiling section.

Because the tunnel route is located in the active NAFZ, the need for an intermediate lining between the outer and inner linings has arisen. An intermediate lining is installed immediately after the outer lining, approximately 40 m behind the tunnel face. This situation both prevents primary deformations and can bear the cross-sectional effects that may occur during an earthquake. The deformation trend is also checked carefully to prevent large plastic zones during construction. Otherwise, the plastic zone is enlarged to the whole overburden, and the unexpected loads affect the lining. In the low overburden section, if the deformations in the tunnel face increase unexpectedly, this is reflected up to the surface and caused by the face collapse in the tunnel. Hence, all the face supports should be installed before the tunnel excavation.

In addition, joint gaps are left between the inner lining in the fault zones encountered during tunnel excavation. Thus, possible displacements in the event
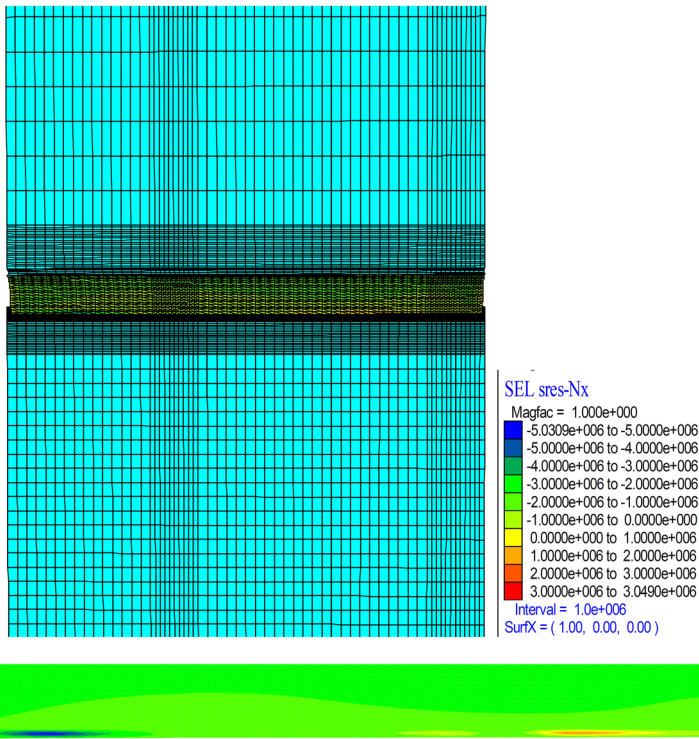
Fig. 28 Axial forces for $h = 90$ m

of an earthquake are damped with these joints. In addition, drainage holes are drilled on the intermediate lining to prevent water loading on the tunnel lining.

Both the intermediate lining and the inner lining installations must be completed in a short time because, in the case of a possible earthquake, in the tunnels
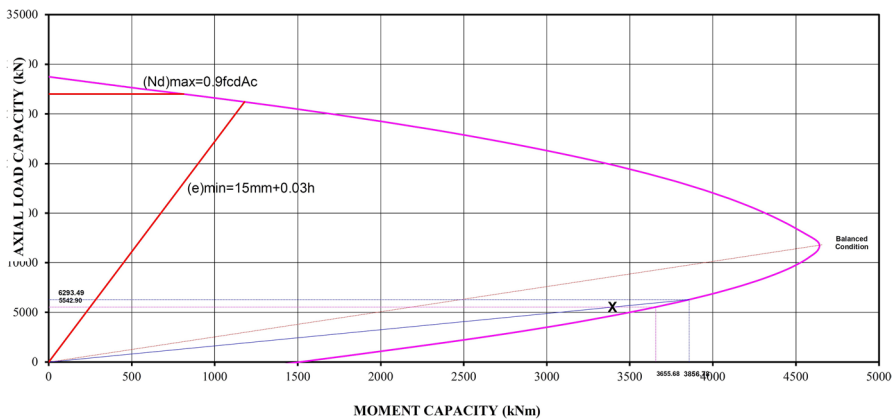

Fig. 29 Interaction diagram in the *X*-direction for the 90 m overburden

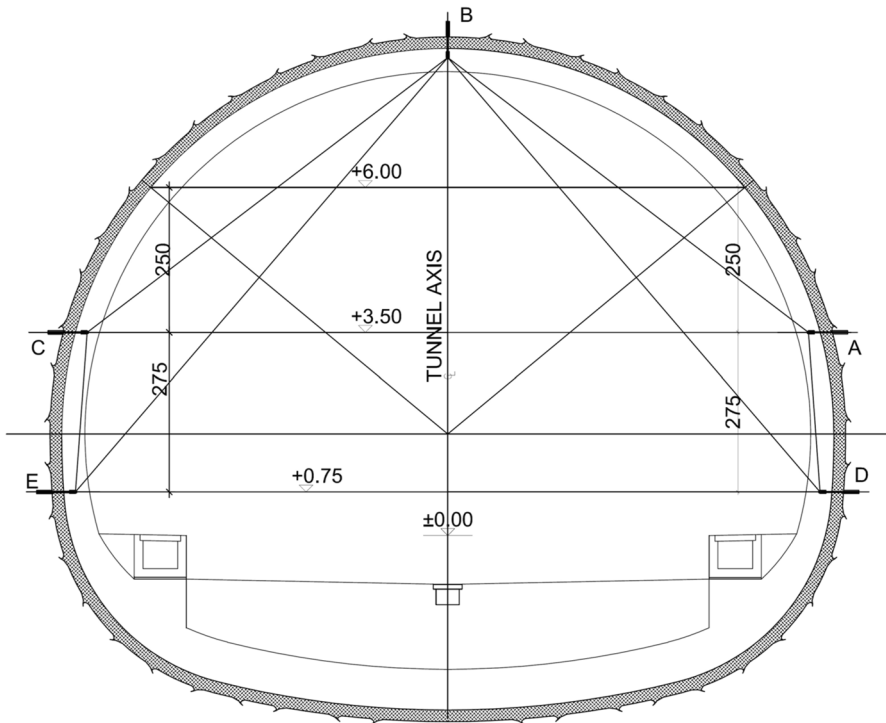**Fig. 30** Intermediate lining applications in the tunnel

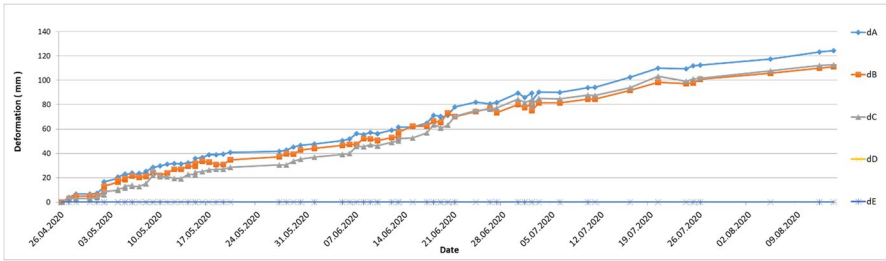**Fig. 31** Deformation measurement points in the tunnel section

Fig. 32 Deformation measurement at km: 124 + 677 before the intermediate lining application

where only the outer lining is completed, the lining cannot carry the load and resulting in collapse.

As seen from the analysis results, for the 30 m overburden, a 20-cm deformation occurred in the *Y*-direction, that is, in the tunnel face, towards the inside of the tunnel in cohesionless units. A 65-cm deformation (in total) occurs in the **Z**-direction (the vertical direction). In the analyses for clayey units ($h = 60$ m), a total vertical deformation of up to 5 cm and a displacement of up to 8 cm in the tunnel face are observed. For the 90-m overburden height, vertical deformation of up to 8 cm and deformation of up to 16 cm in the *Y*-direction (tunnel face) occurs. Deformations in the tunnel face continue upwards in sandy units due to the cohesionless character. In clayey units, deformations are concentrated only in the center of the tunnel face due to the cohesive nature of the ground. The deformations are stabilized at nearly 10 cm in the FLAC3D analysis. The deformations measured in situ are compatible with the numerical analysis; that is, the vertical deformations are less than 10 cm for the 30-m overburden. The deformation observed in the tunnel is nearly 14 cm in the cohesionless soil. Analysis results for the face and umbrella support section, the deformations in the *Z*-direction after excavation in cohesionless units ($h = 30$ m) of the tunnel ceiling decreased to 10 cm, and the deformations in the *Y*-direction decreased to 2.75 cm. In clay units ($h = 60$ m), the deformations in the *Y*-direction in the tunnel decrease to 5 cm after the application of umbrella and cable bolts. Under the 90-m overburden, the deformations decrease to 8 cm in the *Y*-direction and 7 cm in the *Z*-direction.
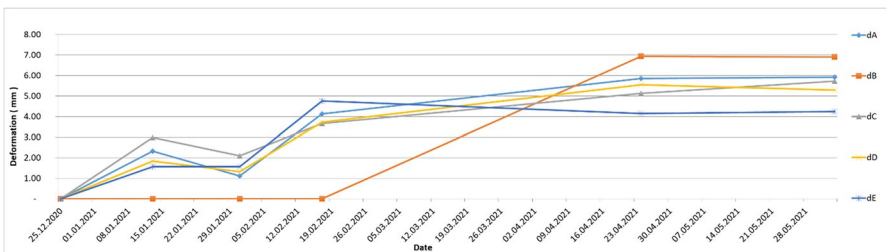

Fig. 33 Deformation measurements at km: 124 + 685 after intermediate lining application

As seen from the analysis results, the face support has a significant effect on tunnel stability. Vertical deformations exceeding 60 cm in cohesionless soils without face supports decrease to 10 cm with face supports for the 30-m overburden thickness. This is extremely important for tunnel stability. For the dynamic analysis, the only outer lining could not resist the earthquake loads so the intermediate lining is necessary. The bending moments and axial force occurring under 60 m of overburden thickness are 2.78×10^6 Nm and 5.78×10^6 N. The cross-sectional effects determined in the analyses performed under an overburden thickness of 90 m, the bending moment and axial force calculated as 3.09×10^6 Nm 5.04×10^6 N, respectively. In the analyses performed according to the section effects, it is determined that the intermediate lining governs the section effects.

This study is a tunnel case excavated in difficult geotechnical and geological conditions, and the methodology followed herein can be applied in similar ground conditions. The tunnel excavations to be carried out in an active earthquake zone are of serious importance. For this reason, geotechnical instruments, such as pressure cells and strain gauges, should be placed inside the inner lining and intermediate lining, and the loads on the lining should be monitored continuously.

Although the analytical solutions provide good results, it is evident that this methodology is insufficient when a tunnel is constructed in difficult ground conditions because the analytical solutions accept homogeneous and isotropic ground conditions. However, it is possible to describe the ground conditions and excavation stages in 3D numerical analyses. In other words, considering the in situ deformation measurements, the 3D numerical analyses give more realistic results while the analytical solutions produce more conservative results.

Declarations

References

Adoko, A.C., Gokceoglu, C., Yagiz, S.: Bayesian prediction of TBM penetration rate in rock mass. Eng. Geol. **226**, 245–256 (2017). https://doi.org/10.1016/j.enggeo.2017.06.014

Agbay, E., Topal, T.: Evaluation of twin tunnel-induced surface ground deformation by empirical and numerical analyses (NATM part of Eurasia tunnel, Türkiye). Comput Geotech **119**, 103367 (2020). https://doi.org/10.1016/j.compgeo.2019.103367

Akgün, H., Muratlı, S.W., Koçkar, M.K.: Geotechnical investigations and preliminary support design for the Geçilmez tunnel: a case study along the Black Sea coastal highway, Giresun, northern Turkey. Tunn. Undergr. Space Technol. **40**, 277–299 (2014)

Aksoy, C.O., Kantarci, O., Ozacar, V.: An example of estimating rock mass deformation around an underground opening using numerical modelling. Int. J. Rock Mech. Min. Sci. **47**, 272–278 (2010)

Aksoy, C.O., Onargan, T.: The role of umbrella arch and face bolt as deformation preventing support system in preventing building damages. Tunneling and Underground Space Technology **25**, 553–559 (2010)

Aksoy, C.O., Ogul, K., Topal, I., Ozer, S.C., Özacar, V., Posluk, E.: Numerical modeling of non-deformable support in swelling and squeezing rock. International Journal of Rock Mechanics and Mining Science **52**, 61–70 (2012)

Aksoy, C.O., Ogul, K., Topal, I., Posluk, E., Gicir, A., Kucuk, K., Uyar Aldas, G.: Reducing deformation effect of tunnel with non-deformable support system by jointed rock mass model. Tunn Underground Space Technol **40**, 218–227 (2014)

Aksoy, C.O., Uyar, G.G., Posluk, E., Ogul, K., Topal, I., Kucuk, K.: Non-deformable support system application at tunnel-34 of Ankara-Istanbul high speed railway project. Structureal Eng Mechanics **58**(5), 869–886 (2016). https://doi.org/10.12989/sem.2016.58.5.869

Alp, M., Apaydin, A.: Assessment of the factors affecting the advance rate of the Tunnel Gerede, the longest and one of the most problematic water transmission tunnels of Turkey. Tunn. Undergr. Space Technol **89**, 157–169 (2019). https://doi.org/10.1016/j.tust.2019.04.001

Apaydin, A.: Comparison of predicted and actual states in tunnels lessons to be learned from the Gerede Water Transmission Tunnel, Türkiye. Quart J Eng Geol Hydrogeol **54**(1), (2021). https://doi.org/10.1144/qjegh2020-060

Armaghani, D.J., Mohamad, E.T., Hajihassani, M., Yagiz, S., Motaghedi, H.: Application of several non-linear prediction tools for estimating uniaxial compressive strength of granitic rocks and comparison of their performances. Eng Computers **32**(2), 189–206 (2016). https://doi.org/10.1007/s00366-015-0410-5

Aydin, A., Ozbek, A., Cobanoglu, I.: Tunnelling in difficult ground: a case study from Dranaz tunnel, Sinop. Türkiye. Eng Geol **74**(3–4), 293–301 (2004). https://doi.org/10.1016/j.enggeo.2004.04.003

Aygar, E.: Evaluation of new Austrian tunnelling method applied to Bolu tunnel's weak rocks. J Rock Mechanics Geotech Eng **12**, 541–556 (2020). https://doi.org/10.1016/j.jrmge.2019.12.011

Aygar, E.B., Gokceoglu, C.: Problems encountered during a railway tunnel excavation in squeezing and swelling materials and possible engineering measures: a case study from Türkiye. Sustainability **12**(3), 1166 (2020). https://doi.org/10.3390/su12031166

Aygar, E.B., Gokceoglu, C.: Analytical solutions and 3D numerical analyses of a shallow tunnel excavated in weak ground: a case from Turkey. Geo-Engineering **12**, 9 (2021). https://doi.org/10.1186/s40703-021-00142-7

Aygar, E.B., Gokceoglu, C.: A special support design for a large-span tunnel crossing an active fault (T9 Tunnel, Ankara-Sivas High-Speed Railway Project, Turkey). Environ Earth Sci **80**(1), 37 (2021). https://doi.org/10.1007/s12665-020-09328-1

Aygar, E.B., Gokceoglu, C.: An assessment on the inner lining need for a large-span tunnel (a case from Turkey, Akyazi Tunnel, Trabzon). SN Appl Sci **3**(4), 457 (2021). https://doi.org/10.1007/s42452-021-04366-1

Barton, N.: Minimizing the use of concrete in tunnels and caverns: comparing NATM and NMT. Innovative Infrastructure Solutions **2**(1), 52 (2017). https://doi.org/10.1007/s41062-017-0071-x

Barton, N.R., Lien, R., Lunde, J.: Engineering classification of rock masses for the design of tunnel support. Rock Mech. **6**(4), 189–239 (1974)

Bieniawski, Z.T.: Engineering classification of jointed rock masses. Trans s. Afr. Inst. Civ. Engrs **15**, 335–344 (1973)

Bieniawski, Z.T.: Engineering rock mass classifications. Wiley, New York (1989)

Bilgin, N.: An appraisal of TBM performances in Turkey in difficult ground conditions and some recommendations. Tunnelling and Underground Space Technology **57**, 265–276 (2016). https://doi.org/10.1016/j.tust.2016.01.038

Bilgin, N., Algan, M.: The performance of a TBM in a squeezing ground at Uluabat, Türkiye. Tunn. Undergr. Space Technol. **32**, 58–65 (2012). https://doi.org/10.1016/j.tust.2012.05.004

Bilgin, N., Ates, U.: Probe drilling ahead of two tbms in difficult ground conditions in Türkiye. Rock Mech. Rock Eng. **49**(7), 2763–2772 (2016). https://doi.org/10.1007/s00603-016-0937-9

Bilgin, N., Acun, S.: The effect of rock weathering and transition zones on the performance of an EPB-TBM in complex geology near Istanbul, Türkiye. Bull. Eng. Geol. Env. **80**(4), 3041–3052 (2021). https://doi.org/10.1007/s10064-021-02142-4

Cao, C., Shi, C., Lei, M., Yang, W., Liu, J.: Squeezing failure of tunnels: a case study. Tunn. Undergr. Space Technol. **77**, 188–203 (2018). https://doi.org/10.1016/j.tust.2018.04.007

Cao, H., Peng, L., Lei, M., Tang, Q., Peng, L., Chen, F.: Calculation model of supporting system for tunnel under shallow and weak surrounding rock considering the synergistic effects. Geotech Geol Eng **38**, 1379–1388 (2020). https://doi.org/10.1007/s10706-019-01097-4

Das, R., Singh, P.K., Kainthola, A., Panthee, S.: Numerical analysis of surface subsidence in asymmetric parallel highway tunnels. J Rock Mech Geotech Eng **9**(2017), 170–179 (2017)

Dalgic, S.: Tunneling in squeezing rock, the Bolu tunnel, Anatolian Motorway, Türkiye. Eng. Geol. **67**, 73–96 (2002)

Dalgic, S.: Tunneling in fault zones, Tuzla tunnel, Türkiye. Tunn. Undergr. Space Technol. **18**(5), 453–465 (2003). https://doi.org/10.1016/S0886-7798(03)00045-2

Eftekhari, A., Aalianvari, A.: An overview of several techniques employed to overcome squeezing in mechanized tunnels a case study. Geomech Eng **18**(2), 215–224 (2019). https://doi.org/10.12989/gae.2019.18.2.215

Emre, Ö., Erkal, T., Tchepalyga, A., Kazancı, N., Keçer, M., ve Ünay, E.: Neogene-Quaternary evolution of the eastern Marmara region. Northwest Türkiye: Mineral Res Ve Exploration Bull **120**, 119–145 (1998)

Farrokh, E., Rostami, J.: Effect of adverse geological condition on TBM operation in Ghomroud tunnel conveyance project. Tunn. Undergr. Space Technol. **24**(4), 436–446 (2009). https://doi.org/10.1016/j.tust.2008.12.006

Hasanpour, R., Rostami, J., Thewes, M., Schmitt, J.: Parametric study of the impacts of various geological and machine parameters on thrust force requirements for operating a single shield TBM in squeezing ground. Tunn. Undergr. Space Technol. **73**, 252–260 (2018). https://doi.org/10.1016/j.tust.2017.12.027

Hashash, Y.M.A., Hook, J.J., Schmidt, B., Yao, J.I.: Seismic design and analysis of underground structures. Tunneling and Underground Space Technology **16**, 247–293 (2001)

Hoek, E., Brown, E.T.: Underground excavations in rock. Instn Min. Metall, London (1980)

Kargar, A.R., Rahmannejad, R., Hajabasi, M.A.: A semi-analytical elastic solution for stress field of lined non-circular tunnels at great depth using complex variable method. Int. J. Solids Struct. **51**(6), 1475–1482 (2014). https://doi.org/10.1016/j.ijsolstr.2013.12.038

Kaya, A., Bulut, F.: Geotechnical studies and primary support design for a highway tunnel: a case study in Türkiye. Bull Eng Geol Envron **78**(8), 6311–6334 (2019). https://doi.org/10.1007/s10064-019-01529-8

Khanbabazadeh, H., Iyisan, R.: A numerical study on the 2D behavior of the single and layered clayey basins. Bulletin of Earthquake Eng **12**, 1515–1536 (2014)

Kirsch, E.G.: The theory if elasticity and the need of the strength of materials (trans.). J Assoc German Eng. **42**, 797–807 (1898)

Koçkar, M.K., Akgün, H.: Methodology for tunnel and portal support design in mixed limestone, schist and phyllite conditions: a case study in Türkiye. Int. J. Rock Mech. Min. Sci. **40**, 173–196 (2003)

Komu, M.P., Guney, U., Kilickaya, T.E., Gokceoglu, C.: Using 3D numerical analysis for the assessment of tunnel-landslide relationship: Bahce-Nurdag Tunnel (South of Türkiye). Geotech. Geol. Eng. **38**(2), 1237–1254 (2020). https://doi.org/10.1007/s10706-019-01084-9

Kong, S.M., Choi, S.I., Shim, S.B., Lee, H., Oh, D.W., Lee, S.W.: Stability evaluation of TBM pilot tunnels to rear blasting using the protection shield. Appl. Sci. **11**(4), 1759 (2021). https://doi.org/10.3390/app11041759

Lee, Y.-Z., Schubert, W.: Determination of the round length for tunnel excavation in weak rock. Tunn Underground Space Technol **23**, 221–231 (2008). https://doi.org/10.1016/j.tust.2007.04.001

Li, W., Zhang, C.P., Zhu, W.J., Zhang, D.L.: Upper-bound solutions for the face stability of a non-circular NATM tunnel in clays with a linearly increasing undrained shear strength with depth. Comput. Geotech. **114**, 103136 (2019). https://doi.org/10.1016/j.compgeo.2019.103136

Luo, Y., Chen, J., Chen, Y., Diao, P., Qiao, X.: Longitudinal deformation profile of a tunnel in weak rock mass by using the back analysis method. Tunnelling and Underground Space Technology **71**, 478–493 (2018). https://doi.org/10.1016/j.tust.2017.10.003

Lysmer, J., Kuhlemeyer, R.L.: Finite dynamic model for infinite media. J Eng Mech **95**(EM4), 859–877 (1969)

Maleki, M.R., Dehnavi, R.N.: Influence of discontinuities on the squeezing intensity in high in-situ stresses (a tunnelling case study; actual evidences and TBM release techniques). Rock Mech. Rock Eng. **51**(9), 2911–2933 (2018). https://doi.org/10.1007/s00603-018-1476-3

Moussaei, N., Sharifzadeh, M., Sahriar, K., Khosravi, M.H.: A new classification of failure mechanisms at tunnels in stratified rock masses through physical and numerical modelling. Tunn. Undergr. Space Technol **91**, 103017 (2019)

Niedbalski, Z., Malkowski, P., Majcherczyk, T.: Application of the NATM method in the road tunneling works in difficult geological conditions - the Carpathian flysch. Tunn. Undergr. Space Technol. **74**, 41–59 (2018). https://doi.org/10.1016/j.tust.2018.01.003

Oke, J., Vlachopoulos, N., Marinos, V.: The pre-support nomenclature and support selection methodology for temporary support systems within weak rock masses. J Geotech Geological Eng **32**(1), 97–130 (2014)

Ozcelik, M.: Criteria for the selection of construction method at the Ovit Mountain Tunnel (Türkiye). KSCE J. Civ. Eng. **20**(4), 1323–1328 (2016). https://doi.org/10.1007/s12205-015-0055-3

Palmström, A.: Recent developments in rock support estimates by the RMi. J Rock Mech Tunnelling Technology **6**(1), 1–19 (2000)

Palmström, A.: Combining the RMR, Q, and RMi classification systems. Tunn Underground Space Technol **24**(4), 491–492 (2009)

Panthi, K.K., Basnet, C.B.: Evaluation of earthquake impact on magnitude of the minimum principal stress along a shotcrete lined pressure tunnel in Nepal. J Rock Mech Geotech Eng. **11**, 920–934 (2019)

Sakcali, A., Yavuz, H.: Estimation of radial deformations around circular tunnels in weak rock masses through numerical modelling. Int. J. Rock Mech. Min. Sci. **123**, 104092 (2019). https://doi.org/10.1016/j.ijrmms.2019.104092

Satici, O., Topal, T.: Assessment of damage zone thickness and wall convergence for tunnels excavated in strain-softening rock masses. Tunn. Undergr. Space Technol **108**, 103722 (2021). https://doi.org/10.1016/j.tust.2020.103722

Song, J.S., Yoo, C.S.: Development of knowledge-based study on optimized NATM lining design system. J Korean Geosynthetic Soc **17**(4), 251–265 (2018). https://doi.org/10.12814/jkgss.2018.17.4.251

Sulem, J., Panet, M., Guenot, A.: An analytical solution for time-dependent displacements in a circular tunnel. Int J Rock Mechanics, Mining Sci Geomechanics Abstracts **24**, 155–164 (1987)

Swannell, N., Palmer, M., Barla, G., Barla, M.: Geotechnical risk management approach for TBM tunnelling in squeezing ground conditions. Tunn. Undergr. Space Technol. **57**, 201–210 (2016). https://doi.org/10.1016/j.tust.2016.01.013

Taromi, M., Eftekhari, A., Hamidi, J.K., Aalianvari, A.: A discrepancy between observed and predicted NATM tunnel behaviors and updating: a case study of the Sabzkuh tunnel. Bull. Eng. Geol. Env. **76**(2), 713–729 (2017). https://doi.org/10.1007/s10064-016-0862-x

Vlachopoulos, N., Diederichs, M.S.: Improved longitudinal displacement profiles for convergence confinement analysis of deep tunnels. Rock Mech. & Rock Eng. **42**(2), 131–146 (2009)

Wang, J.-N.: Seismic design of tunnels: a state-of-the-art approach, Monograph, monograph 7. Parsons, Brinckerhoff, Quade and Douglas Inc, New York (1993)

Wang, H.N., Zeng, G.S., Jiang, M.J.: Analytical stress and displacement around non-circular tunnels in semi-infinite ground. Appl. Math. Model. **63**, 303–328 (2018). https://doi.org/10.1016/j.apm.2018.06.043

Wang, X.F., Jiang, B.S., Zhang, Q., Lu, M.M., Chen, M.: Analytical solution of circular tunnel in elastic-viscoplastic rock mass. Latin American J Solids Structures **16**(6), 210 (2019)

Yagiz, S., Gokceoglu, C., Sezer, E., Iplikci, S.: Application of two non-linear prediction tools to the estimation of tunnel boring machine performance. Eng. Appl. Artif. Intell. **22**(4–5), 808–814 (2009). https://doi.org/10.1016/j.engappai.2009.03.007

Yildirim, C., Tuysuz, O.: Estimation of the long-term slip, surface uplift and block rotation along the northern strand of the North Anatolian Fault Zone: inferences from geomorphology of the Almacık Block. Geomorphology **297**, 55–68 (2017). https://doi.org/10.1016/j.geomorph.2017.08.038

Zhang, Q., Li, C., Min, M., Jiang, B.S., Yu, L.Y.: Elastoplastic analysis of circular openings in elasto-brittle-plastic rock mass based on logarithmic strain. Math. Probl. Eng. **2017**, 1–9 (2017)

Zhang, Q., Jiang, B.S., Wu, X.S., Zhang, H.Q., Han, L.J.: Elasto-plastic coupling analysis of circular openings in elasto-brittle-plastic rock mass. Theoret. Appl. Fract. Mech. **60**, 60–67 (2012)

Zhang, Q., Jiang, B.S., Wang, S.L., Ge, X.R., Zhang, H.Q.: Elasto-plastic analysis of a circular opening in strain-softening rock mass. Int. J. Rock Mech. Min. Sci. **50**, 38–46 (2012)

Zhang, Z.Q., Shi, X.Q., Wang, B., Li, H.Y.: Stability of NATM tunnel faces in soft surrounding rocks. Comput. Geotech. **96**, 90–102 (2018). https://doi.org/10.1016/j.compgeo.2017.10.009

Zhang, Q., Zhang, C.H., Jiang, B.S., Li, N., Wang, Y.C.: Elastoplastic coupling solution of circular openings in strain-softening rock mass considering pressure-dependent effect. Int. J. Geomech. **18**, 04017132 (2018)

Zou, J., Chen, G., Qian, Z.: Tunnel face stability in cohesion-frictional soils considering the soil arching effect by improved failure models. Comput. Geotech. **106**, 1–17 (2019)

Barton, N., Løset, F., Lien, R. and Lunde, J. Application of the Q-system in design decisions. In subsurface space, (ed. M. Bergman) **2**, 553–561. New York: Pergamon. (1980)

Bieniawski, Z.T. Rock mass classification in rock engineering. In Exploration for rock engineering, proc. of the symp., (ed. Z.T. Bieniawski) **1**, 97–106. (1976) Cape Town: Balkema.

EWI and WIRKIR,. Tunneling in Moberg Formations, Orkustofnun National Energy Authority. (1972) (https://orkustofnun.is/gogn/Skyrslur/1972/OS-1972-Tunneling-Moberg-2.pdf). Accessed 1 Apr 2019

Fugro Sial.: T1 Tunnel Geological-Geotechnical Investigation Report. Fugro Sial Geosciences Consulting and Engineering Ltd.Ankara. (2019a)

Fugro Sial.: T1 Tunnel Project Report. Fugro Sial Geosciences Consulting and Engineering Ltd.Ankara. (2019b)

Grimstad, E., Barton, N. Updating the Q-System for NMT. Proc. Int. Symp. on sprayed concrete - modern use of wet mix sprayed concrete for underground support, Fagernes. 46–66. (1993) Oslo: Norwegian Concrete Assn.

Hoek, E., Practical Rock Engineering, p 341, (2007) https://www.rocscience.com/assets/resources/learning/hoek/Practical-Rock-Engineering-Full-Text.pdf

Hoek, E., Rock Support Interaction analysis for tunnels in weak rock masses, (2012) https://www.rocscience.com/documents/pdfs/rocnews/winter2012/Rock-Support-Interaction-Analysis-for-Tunnels-Hoek.pdf

Hoek, E. and Marinos, P., 2000. Predicting tunnel squeezing. Tunnels and Tunnelling International. Part 1 – November 2000, Part 2 – December 2000.

Hoek, E., Carranza-Torres, C., Diederichs, M.S., Corkum, B., Integration of geotechnical and structural design in tunnelling. In: Proceedings University of Minnesota 56th Annual Geotechnical Engineering Conference, 29 February 2008. Minneapolis, pp. 1–53. (2008) Available for downloading at Hoek's Corner at <www.rocscience.com>.

Itasca, Flac3d User Manual, Getting Started. (2002)

Kastner, H.. Statics of tunnel and tunnel construction based on geomechanical knowledge. Second revised edition. (1971)

MTA (General Directorate of Mineral Research and Exploration), Geoscience map viewer and drawing editor, yerbilimleri.mta.gov.tr (2021)

Oke, J., Vlachopoulos, N., Diederichs, M.S., Improved input parameters and numerical analysis techniques for temporary support of underground excavations in weak rock. In: RockEng. Edmonton. (2012)

Oke J, Vlachopoulos N, Diederichs MS., The reduction of surface settlement by employing umbrella arch systems. In: GeoMontreal 2013a. Montreal: Canadian Geotechnical Society. (2013a)

Oke J, Vlachopoulos N, Diederichs MS., Modification of the supported longitudinal displacement profile for tunnel face convergence in weak rock. In: 47th US rock mechanics/geomechanics symposium. San Francisco: American Rock Mechanics Association. (2013)

Oke J, Vlachopoulos N, Diederichs MS., Semi-analytical model of an umbrella arch employed in hydrostatic tunnelling conditions. In: 48th US rock mechanics/ geomechanics symposium. Minneapolis: American Rock Mechanics Assoc. (2014)

O'Rourke, T.D., Guidelines for Tunnel Lining Design. ASCE Technical Committee tunn lining design Underground Technol Res Council. (1984)

O'Rourke, T.D., Goh, S.H., Menkiti, C.O., Mair, R.J., Highway tunnel performance during the 1999 Duzce earthquake. Proceedings of the Fifteenth Int Conference Soil Mech Geotech Eng, August 27_31, 2000. Istanbul, Türkiye. (2001)

Owen, G.N., Scholl, R.E., Earthquake engineering of large underground structures. Report no. FHWA_RD-80_195. Federal Highway Administration National Sci Foundation. (1981)

Penzien, J., Seismically -induced racking of tunnel linings. Int. J. Earthquake Eng. Struct. Dyn. 29, 683_691. (2000)

Rabcewicz, L.v., The New Austrian Tunn Method, Part One, Water Power, pp 453–457 (1964)

Rabcewicz, L.v., The New Austrian Tunnelling Method, Part Two, Water Power, pp 511–515 (1964b)

Rabcewicz, L.v., The New Austrian Tunnelling Method, Part Three, Water Power, pp 19–24 (1965)

Sakurai, A., Takahashi, T., Dynamic stresses of underground pipeline during earthquakes. Proceedings of the Fourth World Conference on Earthquake Engineering. (1969)

Terzaghi, K. Rock defects and loads on tunnel supports. In Rock tunneling with steel supports, (eds R. V. Proctor and T. L. White) **1**, 17–99 (1946). Youngstown, OH: Commercial Shearing and Stamping Company.

Yuksel Proje, Karayolu ve Demiryolu Tünelleri ve Diğer Zemin Yapıları (Sektör: Ulaşım Tesisleri – A2) (2019)